Angiopoietin-2 differentially regulates angiogenesis through TIE2 and integrin signaling

Moritz Felcht,[1,2] Robert Luck,[1] Alexander Schering,[1] Philipp Seidel,[1] Kshitij Srivastava,[1] Junhao Hu,[1] Arne Bartol,[1,3] Yvonne Kienast,[4] Christiane Vettel,[5] Elias K. Loos,[1] Simone Kutschera,[1,3] Susanne Bartels,[1] Sila Appak,[1,3] Eva Besemfelder,[1] Dorothee Terhardt,[1] Emmanouil Chavakis,[6] Thomas Wieland,[5] Christian Klein,[4] Markus Thomas,[4] Akiyoshi Uemura,[7] Sergij Goerdt,[2] and Hellmut G. Augustin[1,3]

[1]Division of Vascular Oncology and Metastasis, German Cancer Research Center Heidelberg (DKFZ-ZMBH Alliance), Heidelberg, Germany. [2]Department of Dermatology, Venerology, and Allergology and [3]Department of Vascular Biology and Tumor Angiogenesis (CBTM), Medical Faculty Mannheim, Heidelberg University, Mannheim, Germany. [4]Roche Diagnostics GmbH, Penzberg, Germany. [5]Institute of Experimental and Clinical Pharmacology and Toxicology, Medical Faculty Mannheim, Heidelberg University, Mannheim, Germany. [6]Department of Internal Medicine, Cardiology and Institute of Cardiovascular Regeneration, Centre for Molecular Medicine, Goethe University, Frankfurt am Main, Germany. [7]Division of Vascular Biology, Department of Physiology and Cell Biology, Kobe University Graduate School of Medicine, Kobe, Japan.

Angiopoietin-2 (ANG-2) is a key regulator of angiogenesis that exerts context-dependent effects on ECs. ANG-2 binds the endothelial-specific receptor tyrosine kinase 2 (TIE2) and acts as a negative regulator of ANG-1/TIE2 signaling during angiogenesis, thereby controlling the responsiveness of ECs to exogenous cytokines. Recent data from tumors indicate that under certain conditions ANG-2 can also promote angiogenesis. However, the molecular mechanisms of dual ANG-2 functions are poorly understood. Here, we identify a model for the opposing roles of ANG-2 in angiogenesis. We found that angiogenesis-activated endothelium harbored a subpopulation of TIE2-negative ECs (TIE2^{lo}). TIE2 expression was downregulated in angiogenic ECs, which abundantly expressed several integrins. ANG-2 bound to these integrins in TIE2^{lo} ECs, subsequently inducing, in a TIE2-independent manner, phosphorylation of the integrin adaptor protein FAK, resulting in RAC1 activation, migration, and sprouting angiogenesis. Correspondingly, in vivo ANG-2 blockade interfered with integrin signaling and inhibited FAK phosphorylation and sprouting angiogenesis of TIE2^{lo} ECs. These data establish a contextual model whereby differential TIE2 and integrin expression, binding, and activation control the role of ANG-2 in angiogenesis. The results of this study have immediate translational implications for the therapeutic exploitation of angiopoietin signaling.

Introduction

The growth of new blood vessels (angiogenesis) follows a coordinated genetic program of vascular sprouting, vessel assembly, and organotypic maturation. The VEGF/VEGF receptor and the Notch/Notch ligand pathways control early steps of the angiogenic cascade related to invasive capillary sprouting. A plethora of neurovascular guidance molecules (ephrins, slits, netrins, semaphorins) subsequently initiate 3D vessel assembly and lumen formation. Last, molecules of the angiopoietin, PDGF, and TGF-β families regulate maturation and vascular remodeling.

Among the regulators of vessel maturation, angiopoietin-2 (ANG-2) has a particularly central role (1). It functions as an autocrine-acting, EC-derived antagonistic ligand of the vessel maturation– and remodeling-controlling ANG-1/TIE2 signaling axis. As such, ANG-2, being almost exclusively produced by ECs, functions as a vessel-destabilizing molecule that facilitates the activities of other endothelial-acting cytokines (2, 3). ANG-2 is presently among the most intensely explored target molecules for the development of second-generation antiangiogenic drugs (4–6). Yet its molecular mechanism of action is poorly understood and largely inferred from the phenotype of genetic gain-of-function (GOF) and loss-of-function (LOF) experiments in mice.

ANG-1– and TIE2-deficient mice have largely complementary mid-gestational lethal phenotypes, resulting from defects in vascular remodeling and vessel maturation (7–9). ANG-2–deficient mice have only mild blood vascular defects (2, 10). In contrast, global overexpression of ANG-2 causes a phenotype that is reminiscent of ANG-1 or TIE2 deficiency (9, 11). These genetic studies have established ANG-1 as the nonredundant agonistic TIE2 ligand, whereas ANG-2 is considered as the antagonist of ANG-1/TIE2 signaling. This concept has more recently been supported by genetic and biochemical studies establishing a role for EC-derived ANG-2 as negative regulator of TIE2 phosphorylation (12).

Despite the genetically solidly established negative regulatory role of ANG-2 on TIE2, several studies have also suggested that ANG-2 may stimulate ECs. In contrast to the destabilizing roles of ANG-2 on resting ECs (13, 14), ANG-2 has been shown to act as an antiapoptotic protective factor for stressed ECs (15), which themselves are particularly strong producers of ANG-2 (16, 17). Several groups have recently reported that the ANG-2–positive tumor endothelium harbors a subpopulation of ECs that do not express its receptor TIE2 (18–22). These puzzling differential expression findings for ANG-2 and its receptor TIE2 raise provocative questions on pos-

Authorship note: Robert Luck and Alexander Schering contributed equally to this work.

Conflict of interest: The authors have declared that no conflict of interest exists.

Citation for this article: *J Clin Invest.* doi:10.1172/JCI58832.

sible signaling roles of ANG-2 in the absence of TIE2. Intriguingly, a possible independence of ANG-2 from its receptor TIE2 has circumstantially been suggested by a recent tumor experiment that revealed more profound antitumor effects upon the targeting of ANG-2 compared with the targeting of its receptor TIE2 (6).

Several reports published during the last 10 years have suggested that ANG-2 may bind to and activate integrins in non-ECs (e.g., fibroblasts, myocytes, as well as glioma and breast cancer cells) (23). Integrins are heterodimeric cell surface molecules involved in cell matrix adhesion as well as outside-in and inside-out signaling (24). The integrins $\alpha_v\beta_3$, $\alpha_v\beta_5$, and $\alpha_5\beta_1$ have been characterized as prototypic molecules of angiogenic ECs. Intriguingly, $\alpha_v\beta_3$ integrin has been shown to be expressed by TIE2-negative ECs (22). ANG-2, in turn, has recently been reported to co-immunoprecipitate with $\alpha_5\beta_1$ integrin in ECs under TNF-α stimulation (4). The differential expression pattern of TIE2 and angiogenic integrins in ECs led us to hypothesize that ANG-2 may differentially signal through its cognate receptor TIE2 and through integrins. This study demonstrates TIE2-independent, integrin-dependent functions of ANG-2 in angiogenic ECs. It thereby establishes a model for the context-dependent effects of ANG-2 acting as a vessel-destabilizing molecule in TIE2-expressing ECs and a directly proangiogenic molecule in TIE2-negative angiogenic ECs.

Results

ANG-2 blockade inhibits angiogenesis by interfering with the stalk and the tip cell phenotypes of ECs. Genetic inactivation of ANG-2 in mice leads to persistent hyaloid vessels and perturbed retinal angiogenesis in postnatal mouse pups (2, 10), indicating a role of ANG-2 in active angiogenesis and vessel remodeling and during vessel regression. In order to molecularly define the target cell population of ANG-2 during angiogenesis, we systemically treated newborn mice with the neutralizing ANG-2 antibody LC06 (25–27) and analyzed the effect on the postnatally growing retinal vasculature in 3D whole mounts (Supplemental Figure 1A for the experimental protocol; supplemental material available online with this article; doi:10.1172/JCI58832DS1). ANG-2 neutralization led to pronounced inhibition of centrifugal angiogenesis, characterized by an overall 40% reduction in retinal vessel area (Figure 1, A and B) and a significant reduction in vascular density (Figure 1, C and D). The complexity of the vascular network was markedly reduced, with a significant non-vascularized area in the center of the retinas (Figure 1, E and F, green), significantly reduced number of junctional branch points (Figure 1G), and reduced total number of vessel segments (Figure 1H). The reduction in vessel branch points resulted in significantly longer vessel segments (average vessel segment length in control IgG treated pups, 28.7 μm vs. average vessel segment length in anti–ANG-2 antibody treated mice, 34.4 μm; Figure 1I). Importantly, these effects were independent of the reduction in the total vessel area (Supplemental Figure 1, B–D). ANG-2 neutralization did not just affect remodeling of central retinal blood vessels. It also affected the sprouting of tip cells at the edge of the growing retinal vascular network. (Figure 1J and Supplemental Figures 1E for 3D reconstruction model of the retina). Retinas in ANG-2 antibody–treated mouse pups had significantly reduced numbers of tip cells (Figure 1K) and fewer filopodia per tip cell (Figure 1L). To extend the tip cell phenotype of ANG-2 inhibition to another in vivo model of angiogenesis, we quantitatively assessed tip cells in subcutaneously growing Colo205 tumors. ANG-2 blockade led to a transient reduction in tumor growth (Figure 1M), similar to the recently reported transient reduction in tumor growth in genetically ANG-2–deficient mice (21, 28). While control IgG-treated tumors had abundant numbers of tip cells (Figure 1N), ANG-2 antibody treatment resulted in significantly reduced numbers of intratumoral tip cells (Figure 1, N and O; $P < 0.05$).

Endothelial tip cells downregulate TIE2 expression but strongly express ANG-2. The antiangiogenic effect of the ANG-2 antibody during retinal angiogenesis indicated a dual effect of ANG-2 blockade on outgrowing capillary sprouting (tip cell invasion) as well as on maturing vessel remodeling (stalk cell differentiation) during physiological and pathological angiogenesis. We therefore probed the expression of the receptor TIE2 in postnatal angiogenic and in adult quiescent retinas. ECs in the adult retina were uniformly positive for TIE2 (Figure 2A). Correspondingly, remodeling stalk cells in the postnatal retina (P6) stained positive for TIE2 (Figure 2B, arrow). Surprisingly, angiogenic ECs at the front of invading microvessels expressed barely detectable to negative levels of TIE2 (P6) (Figure 2B, arrowheads), confirming previous reports of the existence of an EC subpopulation with low TIE2 levels in the angiogenic retina (16, 29). Interestingly, the TIE2 downregulation was most prominent in filopodia-rich tip cells (Figure 2B, arrowheads), whereas blunted ECs at the migrating front showed weak but detectable TIE2 expression (Figure 2B, arrowheads with asterisks).

Extending the retinal expression profiling analyses, we next probed for the expression of TIE2 in the angiogenic intratumoral vasculature of human skin tumors and compared it with the expression of TIE2 in the subcutaneous vessels of the adult skin. Microvessels in the skin were uniformly positive for TIE2, whereas the pattern of TIE2 expression in the tumor vasculature was more heterogeneous, with a majority of TIE2-positive ECs, a smaller subpopulation of weakly TIE2-expressing ECs, and some ECs being completely TIE2 negative (Figure 2C). As a third in vivo model for the comparative analysis of TIE2 expression in angiogenic versus quiescent ECs, we analyzed TIE2 in an EC xenotransplantation assay in which a human microvascular network was engineered in immunocompromised mice by grafting human ECs in a 3D matrix (30, 31). In this model, ECs in microvessels with a patent lumen were TIE2 positive, whereas ECs in non-lumenized vascular sprouts were TIE2 negative (Figure 2D).

The pattern of $TIE2^{hi}$ and $TIE2^{lo}$ ECs suggested an association of TIE2 downregulation during active angiogenesis, most notably with the phenotype of angiogenic tip cells. We therefore examined the effect of angiogenic cytokine activation on TIE2 expression in different cellular models of EC activation. FACS analysis of dissociated vascular networks of ECs growing in a 3D cellular model of angiogenesis (32) revealed significantly reduced levels of TIE2 expression during VEGF-induced angiogenic sprouting (Supplemental Figure 2, A and B). Correspondingly, VEGF-stimulated sprouting angiogenesis was associated with reduced *TIE2* mRNA content (Supplemental Figure 2C). This effect was observed in collagen as well as in fibrin matrices and upon VEGF as well as bFGF stimulation (Supplemental Figure 2, D and E). For 2D comparisons of the activated and the quiescent EC phenotype, we studied the expression of TIE2 in monolayers of ECs under angiogenic cytokine stimulation (VEGF, TNF-α, and ANG-2). While ANG-2 stimulation did not alter TIE2 receptor expression, VEGF or TNF-α stimulation resulted in the rapid downregulation of TIE2 cell surface presentation (Supplemental Figure 3, A–C). In order to mimic an invasive front of ECs, we performed lateral scratch

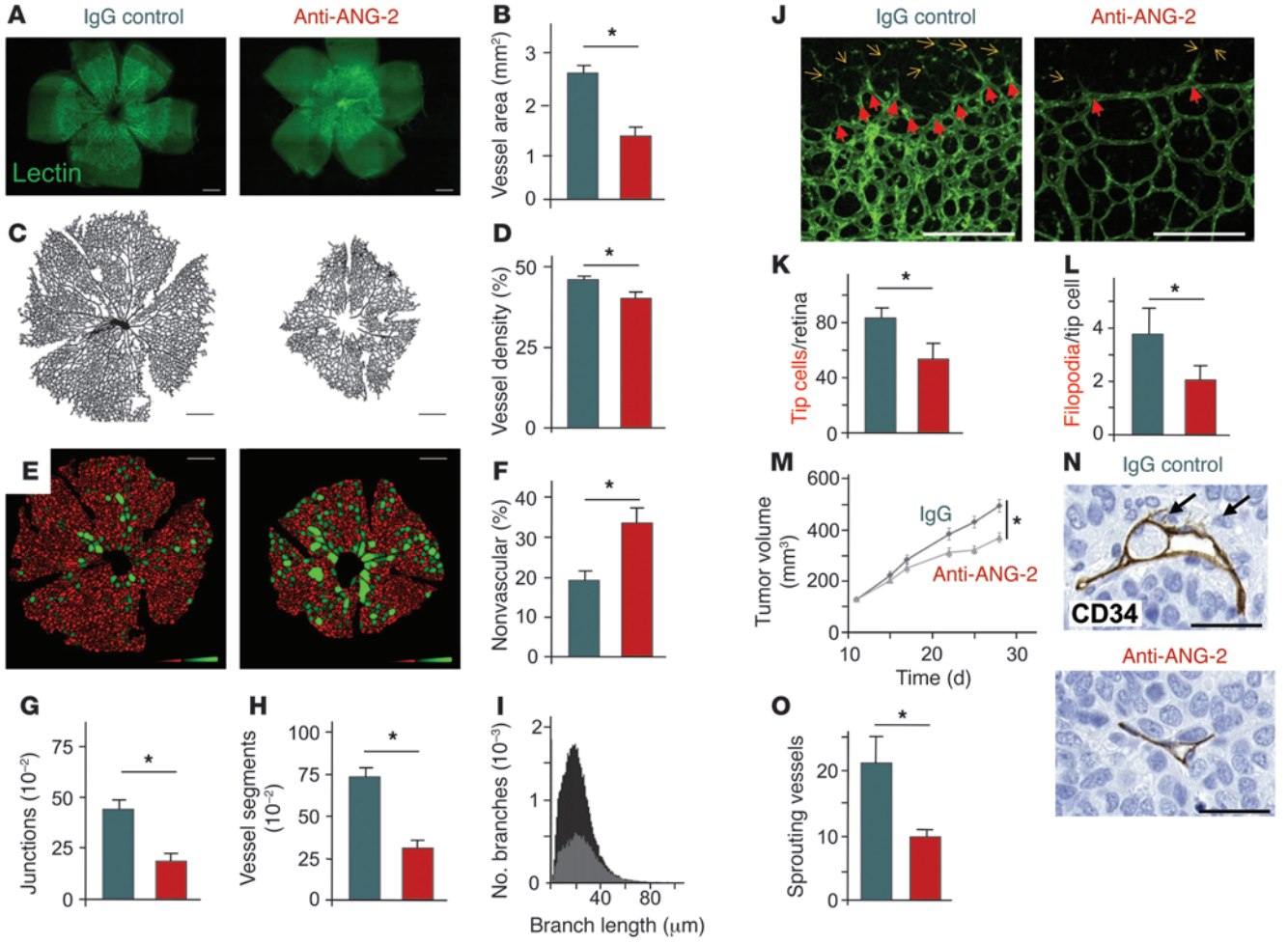

Figure 1

ANG-2 blockage inhibits angiogenesis by interfering with remodeling of the stalk and phalanx cell vasculature as well as by inhibiting the sprouting tip cell EC phenotype. (**A**) Newborn mice were injected intraperitoneally with 30 μg/pup neutralizing ANG-2 antibody (red bars throughout) or IgG control antibody (blue bars) at P1, P3, and P5. Mice were sacrificed at day 6, and the enucleated eyes were processed for retinal whole mount analysis and staining with FITC-labeled lectin (scale bars: 400 μm). (**B**–**I**) Quantitative analysis of the vasculature with Fiji analysis (see Supplemental Experimental Procedures) characterizing the total vessel area (scale bar: 400 μm) (**B** and **C**), the vessel density (**D**), the nonvascularized area (defined as an area that was more than 40 μm away from the next vessel [green]) (scale bars: 400 μm) (**E** and **F**), the junctional branch points per retina (**G**), the vessel segments per retina (**H**), and histogram of the branch length distribution (**I**). For **B**–**H**, $^*P < 0.05$. (**J**–**L**) Higher-resolution images at the edge of the vascular plexus (red arrows, tip cells; yellow arrow, filopodia) demonstrating the pronounced tip cell phenotype–inhibiting effect of the ANG-2 blocking antibody with reduced total number of tip cells/retina (**K**) and fewer filopodia/tip cell (**L**). (**M**–**O**) ANG-2 blockage inhibited tumor growth of subcutaneously growing Colo205 xenografts after anti–ANG-2 treatment ($^*P < 0.05$, mean ± SEM, $n = 20$) (**M**). Colo205 xenograft tumor sections were stained for CD34 and analyzed by high-resolution analysis to detect intratumoral endothelial tip cells (scale bars: 50 μm) (**N**). The number of intratumoral tip cells was significantly reduced in the ANG-2 antibody treatment group ($^*P < 0.05$, mean ± SEM, $n = 5$) (**O**).

wound assays and compared TIE2 expression in unwounded areas with the expression in laterally migrating ECs (Figure 2, E and F). While confluent ECs strongly expressed TIE2, laterally migrating ECs showed significantly reduced TIE2 expression (Figure 2, E and F). In order to characterize the phenotype of the TIE2-negative ECs in more detail, we next performed double-labeling FACS experiments with TIE2 and the established tip cell marker uPAR (16, 17) in confluent and subconfluent ECs (Figure 2, G and H). Interestingly, the TIE2$^-$uPAR$^+$ EC subpopulation was significantly increased in subconfluent cells, indicating that TIE2 is selectively downregulated in tip cells.

The above experiments had indicated that *TIE2* is a negatively regulated gene with constitutive expression by quiescent ECs and downregulated expression by angiogenic ECs. Based on these findings, we probed for expression of the TIE2 ligand ANG-2 in the developing retina. While TIE2 was downregulated in tip cells, ANG-2 expression was strongly upregulated by angiogenic tip cells, confirming and extending earlier studies on ANG-2–positive tip cells (Figure 2I and refs. 16, 17). Comparative analyses of *ANG2* mRNA in confluent and subconfluent EC monolayers similarly revealed that the release of ECs from growth arrest was sufficient to dramatically upregulate *ANG2*

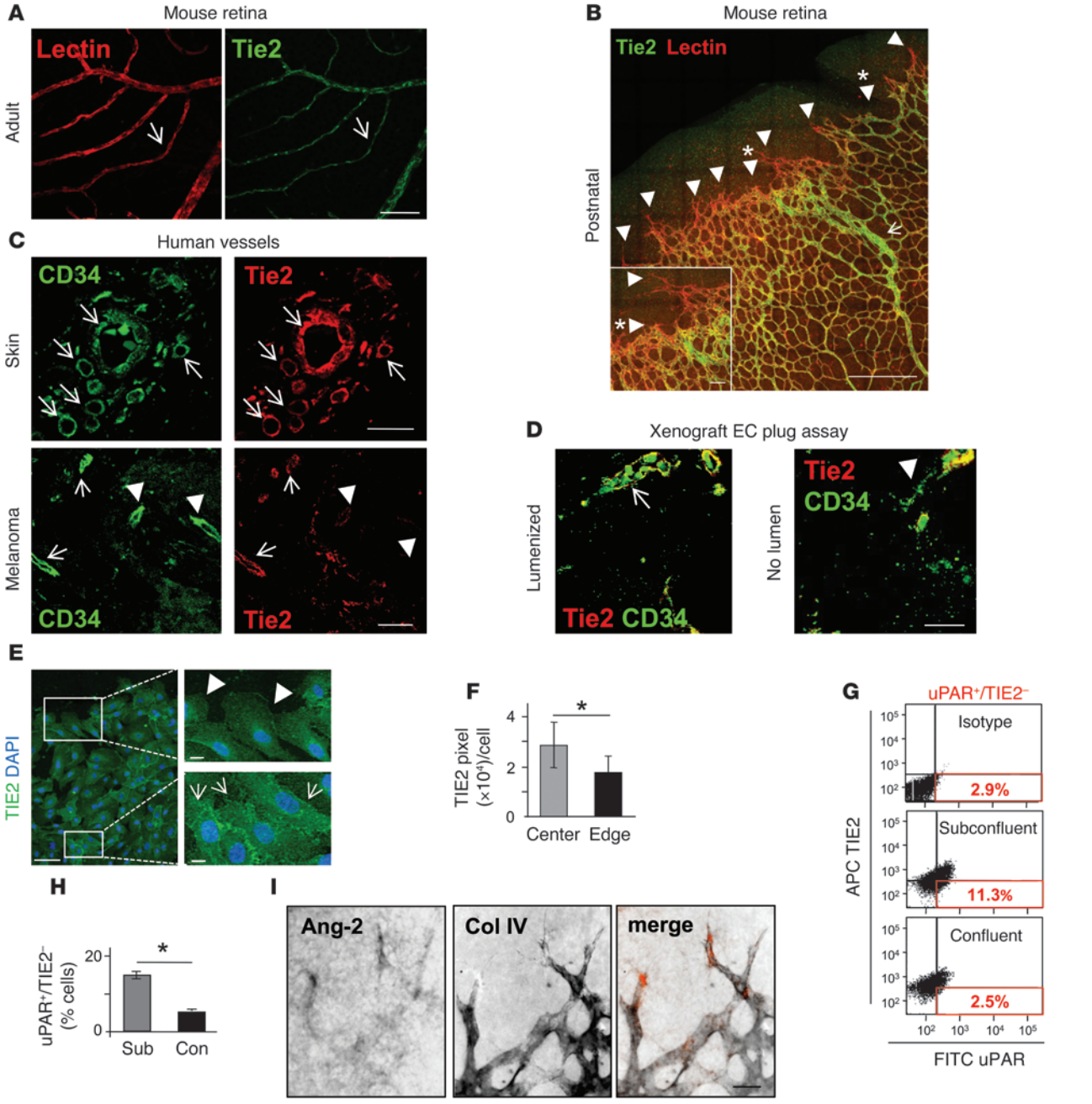

Figure 2

Tip cells have weak TIE2, but strong ANG-2 expression. (**A** and **B**) TIE2 expression in lectin- and TIE2-double-stained retinas from adult mice (**A**) and postnatal mouse pups (**B**) (n = 3 each; arrows: TIE2-positive ECs; arrowheads: TIE2-negative ECs). (**C**) Specimen of human melanoma (n = 6) and healthy skin specimens (n = 3) were stained for CD34 and TIE2. The resting vasculature in the control specimen uniformly coexpressed TIE2 and CD34 (arrows, top row). In contrast, TIE2-positive (arrows) and TIE2-negative ECs (arrowheads) were detected in the vasculature of melanomas (bottom row). (**D**) Co-localization of CD34 and TIE2 in the spheroidal EC xenografting assay (30, 31). Lumenized vessels stained positive for TIE2 (arrow indicating yellow co-localization; left). ECs in non-lumenized vascular structures stained for CD34 but not for TIE2 (arrowhead, right). (**E**) Comparative TIE2 expression of migrating and confluent HUVECs (scratch wound assay; image shown in pseudocolors; n = 3). (**F**) Quantitative assessment of mean TIE2 expression in migrating and confluent ECs (*P < 0.05). (**G**) FACS analysis of confluent and subconfluent ECs for uPAR and TIE2 expression. (**H**) Quantitative assessment of the mean EC subpopulation of TIE2-negative and uPAR-positive ECs under non-permeating conditions. sub, subonfluent; con, confluent. (**I**) Abundant *Ang2* mRNA expression in tip cells of the developing retina. Whole mount retinas were analyzed by in situ hybridization against *Ang2*, followed by immunoreactivity against collagen IV. Merged signals were pseudocolored using Adobe Photoshop CS software. Scale bars: **A**, 75 μm; **B**, 300 μm (insets, 50 μm); **C**, 75 μm; **D**, 75 μm; **E**, 100 μm (insets, 20 μm); **I**, 20 μm.

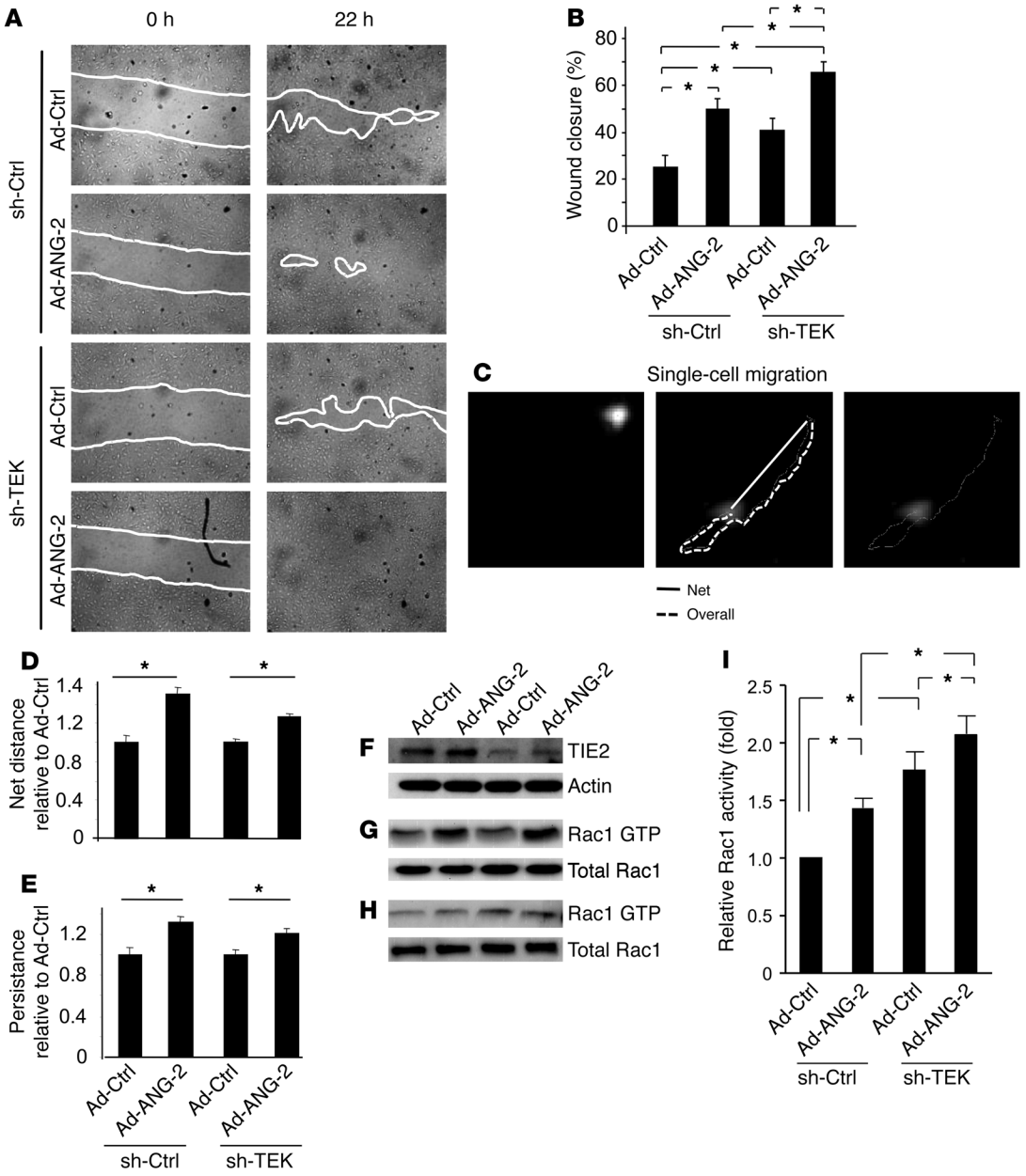

Figure 3

ANG-2 induces Rac activation and migration in TIE2^{lo} ECs. (**A**) Migration of control transduced (sh-Ctrl) and TIE2-silenced ECs (sh-TEK) cotransduced with control adenovirus (Ad-Ctrl) or adenoviral ANG-2 (Ad-ANG-2) in an 18-hour lateral scratch wound migration assay. The white lines denote the wound closure front of migrating ECs. (**B**) Quantification of lateral sheet migration shown in **A** ($n = 3$). The migration-stimulating effect was most pronounced when TIE2 was silenced and ANG-2 overexpressed at the same time. *$P < 0.05$. (**C**) Single-cell migration of control transduced ECs and TIE2-silenced ECs cotransduced with control adenovirus or adenoviral ANG-2. The starting point of individual cells was recorded (top left), and the cells were allowed to migrate for 24 hours (bottom left). The overall distance (dotted line) as well as the net distance (solid line) were recorded (top right). (**D**) Quantification of the net distance of the single-cell tracking assay shown in **C**. Migration of 10 cells per experimental group was expressed as net distance compared with Ad-Ctrl (*$P < 0.05$; $n = 4$). (**E**) Quantification of persistence (net distance divided by overall distance) of the single-cell tracking assay show in **C**. Persistence of 10 cells per experimental group was analyzed and expressed as relative persistence compared to Ad-Ctrl (*$P < 0.05$; $n = 4$). (**F**–**I**) Biochemical analysis of Rac1 activation (Western blot), with quantitative assessment of 7 independent experiments (mean ± SEM; *$P < 0.05$) (**I**). Two representative Western blots are shown (**G** and **H**). TIE2 silencing was monitored by Western blotting (**F**).

mRNA (Supplemental Figure 4A). Likewise, angiogenic activation of ECs in the spheroid sprouting assay by either VEGF or bFGF led to upregulation of *ANG2* mRNA content (Supplemental Figure 4B). Collectively, these data establish a reciprocal regulation of TIE2 and ANG-2 expression in sprouting tip cells compared with remodeling and maturing stalk cells as well as phalanx cells (TIE2^{hi} and ANG-2^{lo} in stalk cells; TIE2^{lo} and ANG-2^{hi} in tip cells).

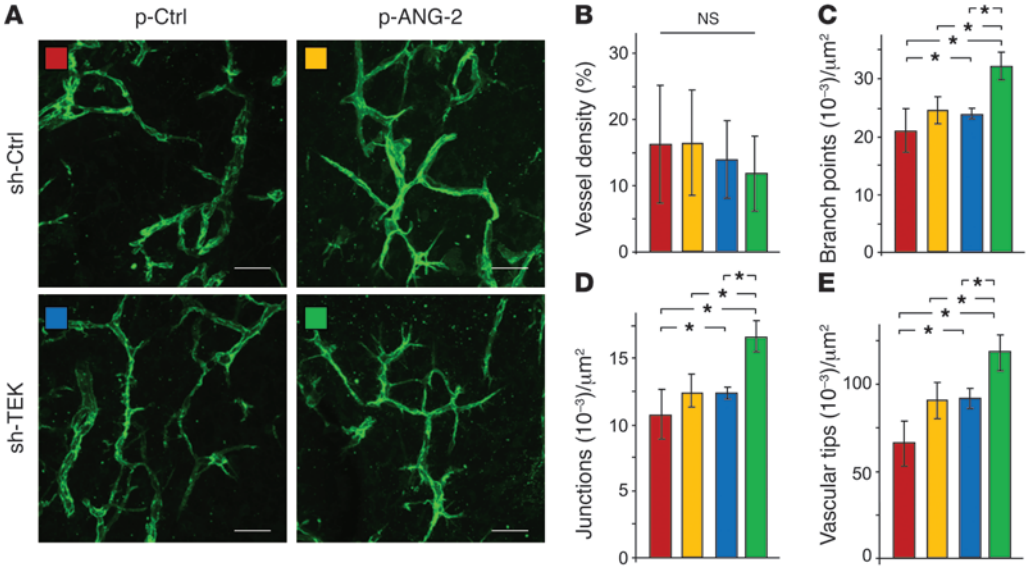

Figure 4
ANG-2 overexpression enhances vascular network formation of TIE2^{lo} ECs. (**A**) Vessel network formation of control transduced and TIE2-silenced ECs cotransduced with control lentivirus (p-Ctrl) or lentiviral ANG-2 (p-ANG-2) in the Matrigel xenografting assay was analyzed as described previously (30, 31). Sections (50 μm) were stained for CD31 and analyzed by Fiji software for mean vessel density (**B**), branch points (**C**), junctions (**D**), and vascular tips (**E**). Red bars indicate sh-Ctrl/p-Ctrl; yellow bars, p-ANG-2/sh-Ctrl; blue bars, p-Ctrl/sh-TEK; green bars p-ANG-2/sh-TEK ECs (*P < 0.05; mean ± SEM; $n \geq 3$). Scale bars: 70 μm.

ANG-2 induces EC migration in TIE2^{lo} ECs. The observed effects of ANG-2 inhibition on sprouting and remodeling ECs during angiogenesis in combination with the reciprocal expression of TIE2 and ANG-2 during angiogenesis led us to hypothesize that ANG-2 may exert direct proangiogenic effects independent of TIE2. We therefore pursued stimulation experiments in control shRNA-transduced and TIE2 shRNA–silenced human ECs, which overexpressed ANG-2 by lentiviral or adenoviral transduction (Supplemental Figure 5, A and B). A lateral scratch wound assay was employed for this purpose as a surrogate of the invading tip cell phenotype to study whether migration is affected by ANG-2 overexpression or TIE2 silencing. Silencing of TIE2 enhanced EC migration (Figure 3, A and B). Similarly, adenoviral overexpression of ANG-2, mimicking the autocrine-acting overexpression by angiogenic ECs, led to a significant enhancement of EC migration (Figure 3, A and B). Intriguingly, though, the strongest effect on EC migration was observed when TIE2 expression was silenced and ANG-2 expression was simultaneously upregulated (Figure 3, A and B).

To shed further light on the relationship among EC migration, TIE2 expression, and ANG-2 expression, we pursued single-cell migration assays and quantified cell migration by measuring the net distance that migrating cells had traveled as well as the persistence of cell movement (33). Both quantitative approaches revealed a significant stimulatory effect of autocrine ANG-2 on EC migration (Figure 3, C–E). As expected as a consequence of downregulated TIE2 expression by subconfluent ECs, single-cell migration experiments in TIE2-silenced ECs did not further enhance ANG-2–stimulated EC migration (Figure 3, C–E).

Coordinated activation of the monomeric GTPases of the Rho family, e.g., activation of Rac1 in response to migratory stimuli, is a hallmark of migrating cells. Pull-down assays were therefore performed to measure Rac1 activity in TIE2^{lo} ECs and control ECs with and without autocrine overexpression of ANG-2. In line with the observed stimulatory effect of ANG-2, Rac1 was detected in its activated GTP-bound form in ANG-2–overexpressing ECs (Figure 3, F–H). Importantly, the ANG-2–induced Rac1 activation was further increased by the loss of TIE2.

The above findings were all compatible with a direct effect of ANG-2 on EC migration. Yet to exclude that any of the observed cellular findings may have resulted indirectly, we studied possible effects of ANG-2 on EC apoptosis or necroptosis (Supplemental Figure 6, A–D). Interestingly, ANG-2 overexpression resulted in a significant reduction in EC necrosis that was independent of TIE2 expression (Supplemental Figure 6D). The number of apoptotic ECs did not change (Supplemental Figure 6C). To study whether, conversely, ANG-2 inhibition would directly affect survival, apoptosis, or necrosis in TIE2^{hi} or TIE2^{lo} ECs, we tested the effect of the ANG-2 neutralizing antibody on EC survival (Supplemental Figure 6, E–H). Confirming previous studies on the non-cytotoxicity of the ANG-2 antibody (26), treatment did not impair cell survival (Supplemental Figure 6F), necrosis (Supplemental Figure 6H), or apoptosis (Supplemental Figure 6G). These findings suggest that the protective effect of ANG-2 on ECs is mediated in an intracellular autocrine manner, as has previously been inferred from cellular experiments (13, 14).

ANG-2 induces sprouting angiogenesis and phosphorylates the integrin adaptor protein FAK (Tyr397) in TIE2^{lo} ECs. Based on the observed tip cell inhibitory phenotype of the ANG-2 neutralizing antibody and the induction of TIE2^{lo} EC migration by ANG-2, we next examined the hypothesis that ANG-2 may directly induce sprouting angiogenesis of TIE2-negative EC. Toward this end, we employed a spheroidal in vivo angiogenesis assay, in which ex vivo GOF or LOF manipulated HUVECs are xenografted in immuno-

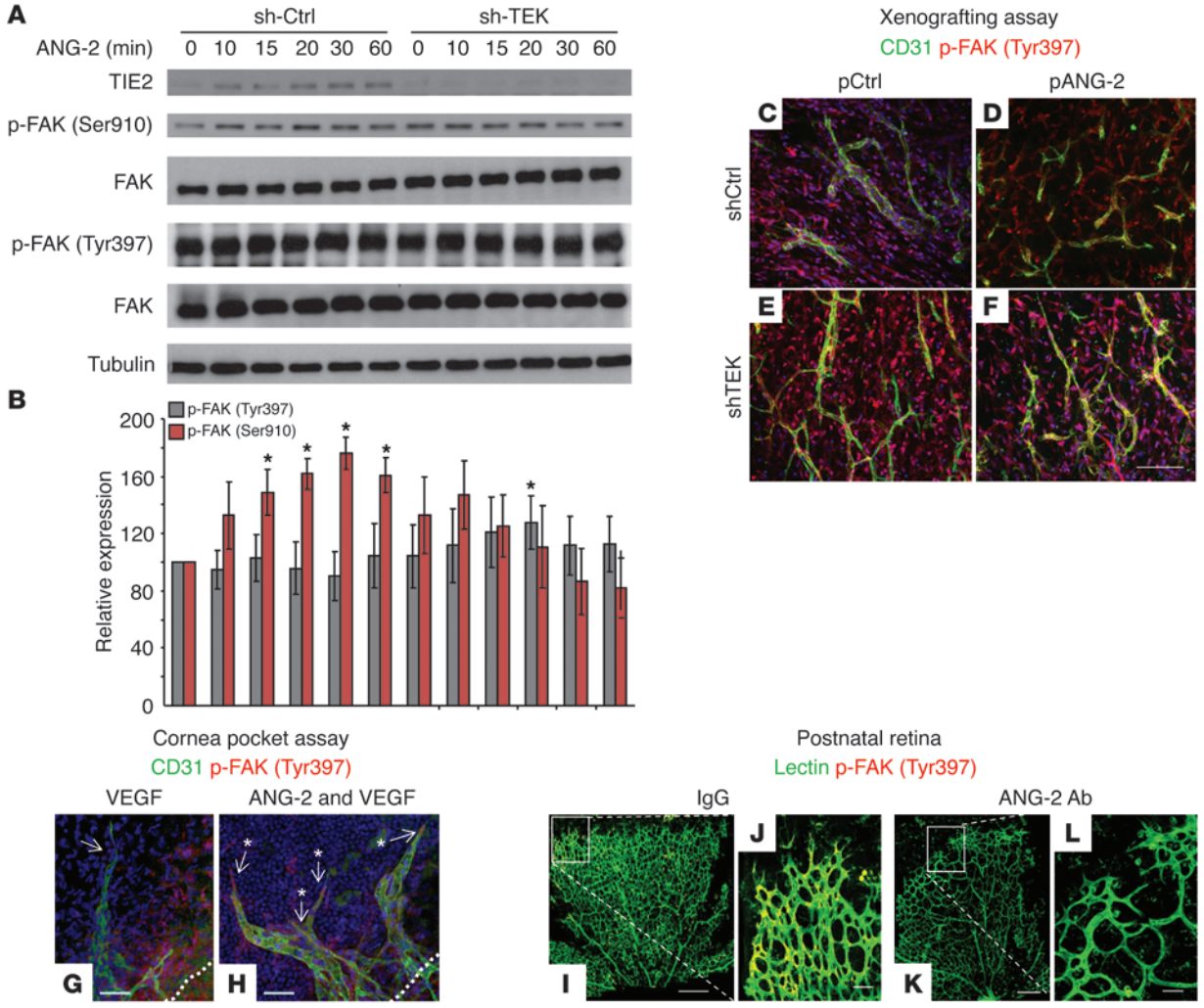

Figure 5

ANG-2 induces in TIE2^{hi} ECs phosphorylation of the integrin adaptor protein FAK at Ser910 and in TIE2^{lo} ECs phosphorylation of FAK at Tyr397. (**A**) Confluent EC monolayers were stimulated with ANG-2. Blots of total cell lysates were probed for FAK phosphorylation at Ser910 (pSer910), Tyr397 (pTyr397), total FAK, and actin or tubulin. (**B**) ImageJ (http://rsb.info.nih.gov/ij/) quantification of FAK phosphorylation at Ser910 or Tyr397 ($n \geq 3$; normalized to tubulin; 1-tailed Student's t test, $^*P < 0.05$). (**C**–**F**) FAK phosphorylation at Tyr397 of control transduced and TIE2-silenced ECs cotransduced with control lentivirus or lentiviral ANG-2 was analyzed in the Matrigel xenografting assay. Sections (50 μm) were stained for CD31 and p-FAK (Tyr397) (Imaris 7.2.3 visualization with pseudocolors). Scale bar: 100 μm. (**G** and **H**) Cornea pocket assay experiments were performed with double implantation of ANG-2 and subcritical doses of VEGF (see Supplemental Figure 8 for an overview of a representative cornea). VEGF-induced sprouting was enhanced by ANG-2 and was accompanied by p-FAK (Tyr397) activity in tip cells (positive: arrows with asterisks; negative: arrow without asterisk). The white dotted line marks the limbus of the cornea. Scale bars: 40 μm. (**I**–**L**) Postnatal mouse pups were systemically treated with ANG-2 blocking antibody (see Supplemental Figure 1A for details), followed by staining for CD31 and p-FAK (Tyr397). Images were taken with z-stack and tilt confocal microscopy. The retinal endothelium strongly expressed p-FAK (Tyr397) (see Supplemental Figure 8B and Supplemental Video 3). Images were assessed with the colocalization function of Imaris 7.2.3. Scale bars: 300 μm for overview (**I** and **K**) and 50 μm for higher-magnification images (**J** and **L**).

compromised mice to give rise to a complex vascular network (30, 31). Grafting of HUVECs with silenced TIE2 expression and ANG-2 overexpression did not result in major changes in the mean vessel density (Figure 4, A and B). Yet network complexity was dramatically altered, with significantly more branch points and blind-ending vascular sprouts (Figure 4, C–E, and Supplemental Figure 7 for 3D visualization). Notably, the combination of ANG-2 overexpression and TIE2 silencing resulted in a filopodia-rich tip cell phenotype, which was not observed in the control groups (Supplemental Videos 1 and 2).

Next, we aimed at characterizing the molecular signaling mechanisms of ANG-2–induced TIE2-independent EC tip cell sprouting. Previous work had shown that ANG-2 stimulated EC destabilization of TIE2-expressing resting ECs involved Ser910 phosphorylation of the integrin adaptor protein FAK (14). When performing the same experiment with TIE2-silenced ECs, we surprisingly saw that ANG-2 stimulation of TIE2^{lo} ECs resulted in FAK phosphorylation at Tyr397, establishing that the absence or presence of TIE2 in ECs resulted in differential FAK phosphorylation upon ANG-2 stimulation (Figure 5, A, and B).

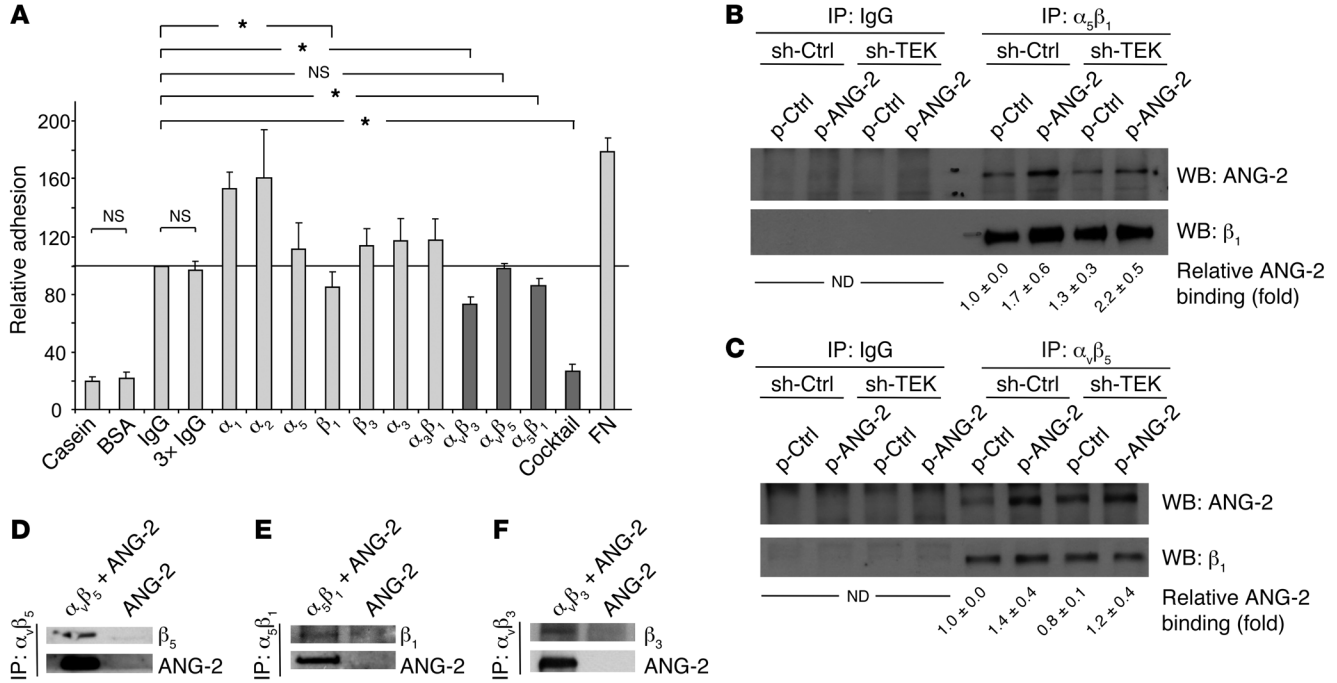

Figure 6

ANG-2 binds $\alpha_v\beta_3$, $\alpha_v\beta_5$, and $\alpha_5\beta_1$ integrins. (**A**) Antibody blocking of HUVEC adhesion to an immobilized ANG-2 matrix. HUVECs were preincubated with the indicated antibodies to integrin monomers and heterodimers (Cocktail: combination of $\alpha_v\beta_3$, $\alpha_v\beta_5$, and $\alpha_5\beta_1$ integrin antibodies), followed by adhesion to an ANG-2 matrix for 40 minutes. Non-adherent cells were removed, and adherent cells were visualized with crystal violet. Color intensities were measured at 550 nm. Antibodies against $\alpha_v\beta_3$, $\alpha_5\beta_1$, and β_1 integrin led to a significant inhibition of HUVEC adhesion to the ANG-2 matrix. Two different β_1 antibodies achieved similar results (*$P < 0.05$ versus IgG; $n = 4$). (**B** and **C**) Control transduced ECs and TIE2-silenced ECs cotransduced with control lentivirus or lentiviral ANG-2 were grown to confluence. Immunoprecipitation for $\alpha_v\beta_5$ and $\alpha_5\beta_1$ or control IgG was performed, followed by SDS-PAGE and detection of ANG-2 by Western blot analysis (upper blots). The membranes were stripped and probed for expression of the integrin monomer (lower blots). The intensity was measured by ImageJ, and the mean of at least 3 independent experiments was calculated. ND, not determined. (**D**–**F**) Interaction of ANG-2 with $\alpha_v\beta_5$ (**D**), $\alpha_5\beta_1$ (**E**), and $\alpha_v\beta_3$ (**F**) in a cell-free co-immunoprecipitation assay. Samples were immunoprecipitated with the indicated integrin antibodies, and co-immunoprecipitation of ANG-2 was probed by Western blotting.

In order to study whether the ANG-2–mediated FAK (Tyr397) phosphorylation in TIE2^{lo} ECs could also be detected in vivo, we performed high-resolution p-FAK (Tyr397) expression analyses in the spheroid xenotransplant angiogenesis assay employing ANG-2 GOF and TIE2^{lo} HUVECs. p-FAK (Tyr397) was weakly detectable in control grafted vascular networks (Figure 5C). In turn, grafting of ECs with silenced TIE2 expression and simultaneous ANG-2 overexpression induced pronounced phosphorylation of FAK (Tyr397) (Figure 5, D–F). Importantly, p-FAK (Tyr397) was most abundantly detectable in sprouting, non-lumenized ECs (Figure 5, C–F).

Complementing the xenografting experiments, we employed the cornea pocket assay as a second in vivo angiogenesis model. ANG-2 alone did not induce vascular sprouting (Supplemental Figure 8A), and low concentrations of VEGF (80 ng) similarly induced only a weak angiogenic response (Figure 5G and Supplemental Figure 8A). Yet the combination of low VEGF and ANG-2 induced a robust angiogenic response (Figure 5H and Supplemental Figure 8A). High-resolution immunofluorescence revealed most pronounced detection of p-FAK (Ty397) in blind-ending tip cells (Supplemental Video 3).

As a third in vivo model, we analyzed p-FAK (Tyr397) expression during postnatal retinal angiogenesis in mouse pups treated with the ANG-2 neutralizing antibody. Strong p-FAK (Tyr397) phosphorylation was detectable in postnatal retinal whole mounts (Figure 5, I and J). Treatment with the ANG-2 blocking antibody essentially abrogated p-FAK (Tyr397) staining in the angiogenic retina (Figure 5, K and L).

ANG-2 binds $\alpha_v\beta_3$, $\alpha_v\beta_5$, and $\alpha_5\beta_1$ integrins with lower affinity than TIE2. Several reports have independently suggested the binding of ANG-2 by integrins expressed by different cell populations, including fibroblasts, myocytes, monocytes, and tumor cells (23, 34–37). Recently, similar findings have been reported for ECs (38). While the binding of ANG-2 by integrins appears to be solidly established, no work has been done so far to unravel the functional relevance in regulating EC behavior. The experiments performed in this study had indicated a direct proangiogenic effect of ANG-2 on TIE2^{lo} ECs, which involved the integrin adaptor protein FAK. We therefore decided to systematically study the binding of ANG-2 to EC-expressed integrins with a focus on those integrins that contribute to shaping the angiogenic EC phenotype (39).

Adhesion assays of ECs on immobilized ANG-2 in the presence or absence of neutralizing integrin antibodies revealed binding of ANG-2 to $\alpha_v\beta_3$, $\alpha_5\beta_1$, and β_1 integrins (Figure 6A). The employed antibodies against the α_1, α_2, and α_5 integrin subunits or the $\alpha_v\beta_5$ integrin heterodimer had no effect on EC adhesion to the ANG-2 matrix (Figure 6A). As $\alpha_v\beta_3$, $\alpha_v\beta_5$, and $\alpha_5\beta_1$ integrins can partly

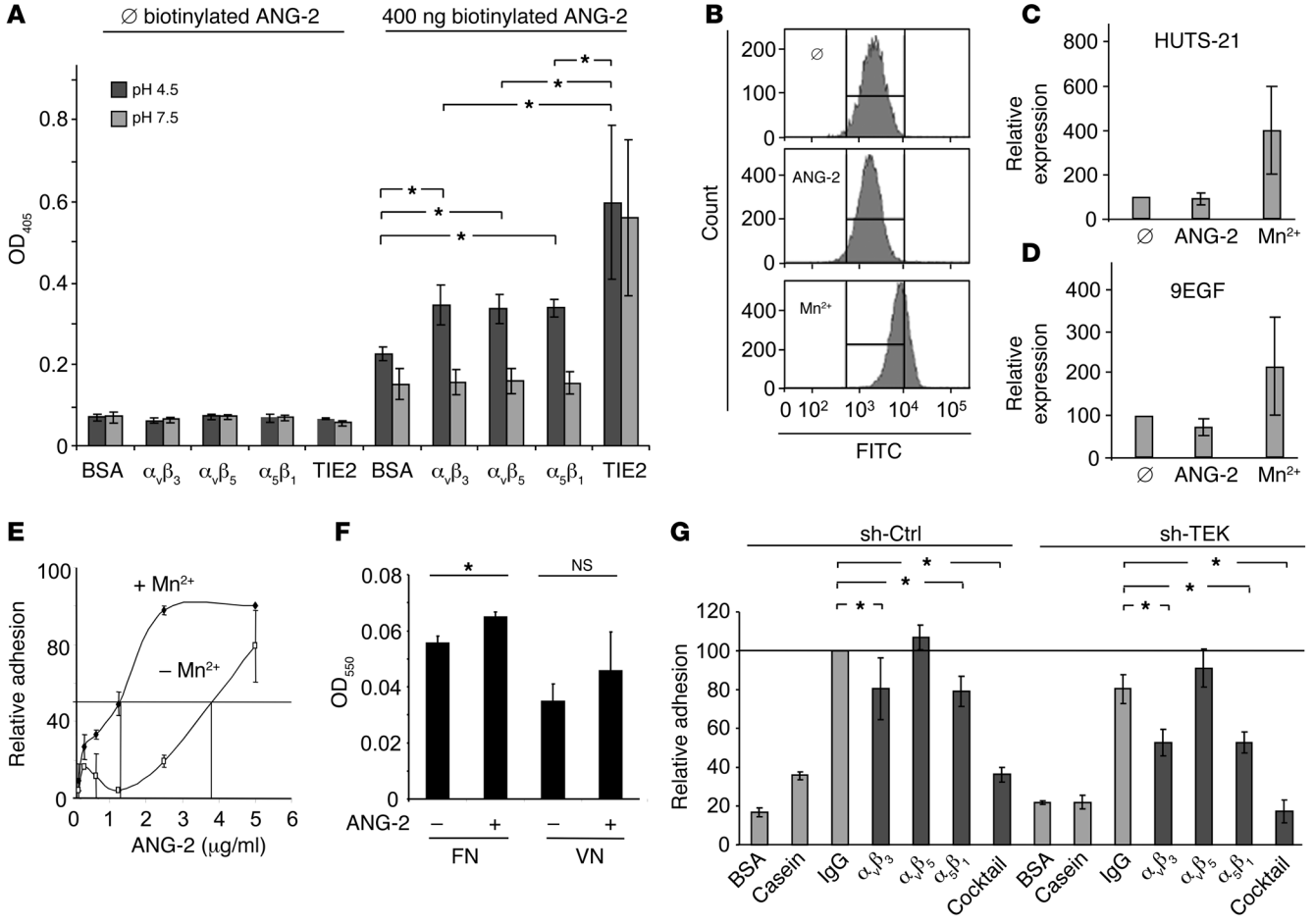

Figure 7

ANG-2 binds to $\alpha_v\beta_3$, $\alpha_v\beta_5$, and $\alpha_5\beta_1$ integrins with lower affinity than TIE2 receptor. (**A**) ELISA quantification of ANG-2 adhesion to TIE2 or integrins at physiological pH or in an acidic environment. ANG-2 bound in an acidic environment with significantly higher affinity to TIE2 compared with the integrin heterodimers (*$P < 0.05$; $n = 3$). (**B**–**D**) HUVEC monolayers were stimulated with Mn^{2+} or ANG-2. The integrin conformation was studied with β_1 integrin active conformation antibodies (HUTS-21, 9EGF) (40, 41). The mean intensity was determined and the relative conformation expression quantified ($n = 3$). In contrast to Mn^{2+} stimulation, ANG-2 did not induce conformational changes in β_1 integrins. (**E**) Effect of Mn^{2+} on HUVEC adhesion to immobilized ANG-2. HUVECs adhered to ANG-2–coated plates with or without Mn^{2+}. Adherent cells were visualized with crystal violet. (**F**) Competition binding of ANG-2 and RGD-containing proteins. After preincubation of ECs with ANG-2, cells adhered to plates coated with fibronectin (FN) or vitronectin (VN). Adherent cells were visualized with crystal violet. Preincubation with ANG-2 did not reduce binding to RGD-containing FN or VN but enhanced HUVEC adhesion to FN (*$P < 0.05$; $n = 3$). (**G**) Antibody blocking of control transduced and TIE2-silenced HUVEC adhesion to ANG-2. HUVECs were preincubated with the indicated integrin heterodimer antibodies (cocktail: combination of $\alpha_v\beta_3$, $\alpha_v\beta_5$, and $\alpha_5\beta_1$ integrin antibodies), followed by adhesion to ANG-2. Adherent cells were visualized with crystal violet. Antibodies against $\alpha_v\beta_3$, $\alpha_5\beta_1$, and the integrin cocktail inhibited HUVEC adhesion to the ANG-2 matrix to baseline levels in $TIE2^{lo}$ ECs (*$P < 0.05$; $n = 3$).

compensate for each other (40), a cocktail against all three integrins was also applied. The strongest adhesion-blocking effect was exerted with the mixture of $\alpha_v\beta_3$, $\alpha_v\beta_5$, and $\alpha_5\beta_1$ integrin antibodies (Figure 6A). Based on these findings, we performed direct ANG-2/integrin co-immunoprecipitation experiments with $TIE2^{lo}$ ECs overexpressing ANG-2 (Figure 6, B and C). ANG-2 directly associated with $\alpha_5\beta_1$ and $\alpha_v\beta_5$ integrins in ECs (Figure 6, B and C). Immunoprecipitation of $\alpha_v\beta_3$ did not reveal direct binding of ANG-2 in this cellular setting. In order to determine whether ANG-2 can directly associate with $\alpha_v\beta_5$ and $\alpha_5\beta_1$ integrins without involvement of adaptor proteins, we performed immunoprecipitation experiments in a cell-free system (Figure 6, D and E). ANG-2 directly associated with $\alpha_v\beta_5$ and $\alpha_5\beta_1$ integrins (Figure 6, D and E). As $\alpha_v\beta_5$ integrin and $\alpha_v\beta_3$ integrin are structurally similar and express redundant binding sites, binding studies were also performed with $\alpha_v\beta_3$ integrin and ANG-2 in this cell-free system (Figure 6F). Indeed, ANG-2 directly associated with $\alpha_v\beta_3$ integrin (Figure 6F).

Hypoxia and an acidic environment accompany the early steps of angiogenesis. Therefore, we performed binding experiments at physiological and acidic pH (Figure 7A). These ELISA-based binding studies confirmed the results of the immunoprecipitation experiments and showed that the three integrins bound to ANG-2 with similar affinity (Figure 7A). Yet in contrast to ANG-2/TIE2 binding, the association between ANG-2 and the integrins required an acidic environment (Figure 7A). However, the affinity of integrin binding to ANG-2 was significantly lower than the binding to TIE2 even at low pH (Figure 7A). Integrin binding and activation may induce

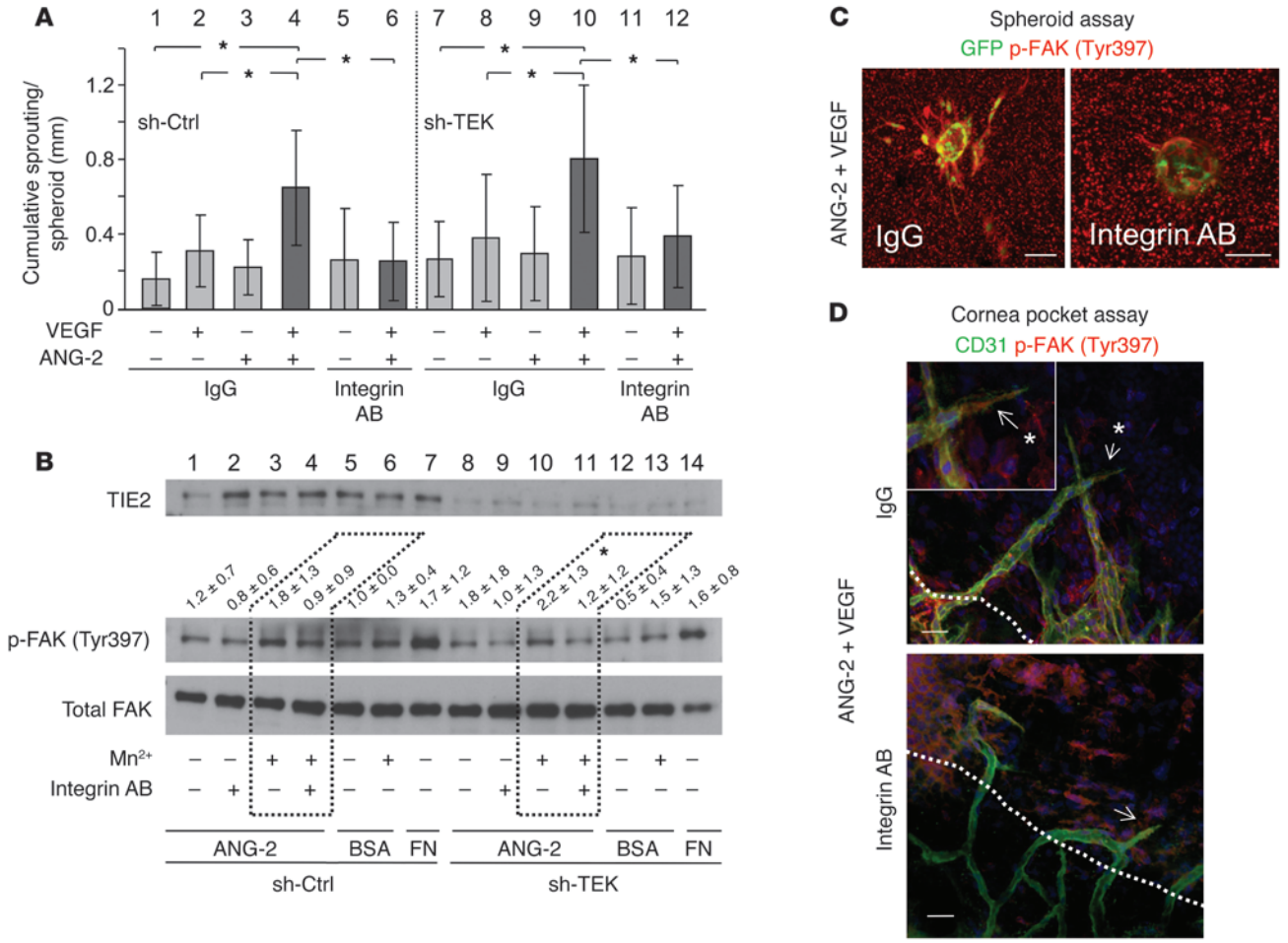

Figure 8

ANG-2–induced enhancement of VEGF sprouting and FAK (Tyr397) phosphorylation require $\alpha_v\beta_3$, $\alpha_v\beta_5$, and $\alpha_5\beta_1$ integrins. (**A**) Spheroid sprouting assay with shRNA control ECs or lentivirally silenced TIE2 ECs in the presence of control IgG or the integrin antibody cocktail against $\alpha_v\beta_3$, $\alpha_v\beta_5$, and $\alpha_5\beta_1$ (Integrin AB). Spheroids were stimulated with VEGF, ANG-2, or a combination of both, and the cumulative sprout length was quantified (*$P < 0.05$; $n = 3$). (**B**) Effect of ANG-2 on p-FAK (Tyr397) activation. Control and TIE2-silenced HUVECs were preincubated with the $\alpha_v\beta_3$, $\alpha_v\beta_5$, and $\alpha_5\beta_1$ integrin antibody cocktail and adhered with or without Mn^{2+} to ANG-2–coated dishes (BSA, negative control; fibronectin, positive control). Blots of adherent and non-adherent cell lysates were probed for TIE2, p-FAK (Tyr397), and total FAK. Dotted boxes mark the effect of integrin blockage on ANG-2–induced p-FAK (Tyr397) (lane 10 versus 11) (ImageJ quantitation; $n = 3$; 1-tailed Student's t test, *$P < 0.05$). (**C**) Spheroid sprouting was induced by ANG-2 and VEGF with IgG control or integrin blocking antibody cocktail in TIE2-silenced ECs. Spheroids were stained for p-FAK (Tyr397) and visualized together with lentiviral GFP by confocal microscopy. (**D**) The cornea pocket assay was performed with IgG control or $\alpha_v\beta_3$, $\alpha_v\beta_5$, and $\alpha_5\beta_1$ antibody blockage. Angiogenesis was induced with ANG-2 and VEGF. The combination of ANG-2 and VEGF induced sprouting in the IgG control and FAK phosphorylation at Tyr397 (upper panel, arrows with asterisk). In contrast, integrin blockage inhibited sprouting and p-FAK (Tyr397) activation (arrow) (white dotted line marks corneal limbus). A higher-magnification image is shown in the inset. Scale bars: 30 μm.

conformational changes in the integrin. Two antibodies are commercially available for study of β_1 integrin conformation (HUTS-21 and 9EGF) (41, 42). We therefore performed FACS experiments to study whether ANG-2 stimulation induces β_1 integrin conformational changes (Figure 7, B–D). While Mn^{2+} stimulation strongly enhanced the active conformation of β_1 integrins, ANG-2 stimulation of ECs did not induce β_1 integrin conformational changes (Figure 7, B–D).

The inserted-like (I-like) domain of integrins is essential for integrin-ligand binding (43). A metal-ion-dependent adhesion site (MIDAS) is localized in the center of the I-like domain. Consequently, divalent cations allow α MIDAS and/or β MIDAS ligand binding to integrins. To examine a possible involvement of integrin MIDAS binding sites in ANG-2 binding, we performed adhesion assays in the presence or absence of the cation Mn^{2+}. Titration of matrix-bound ANG-2 in the EC adhesion assay revealed an adhesion-promoting effect of Mn^{2+}, as evidenced by a shift in the affinity curve (Figure 7E). Together, the inability of ANG-2 to induce a conformational integrin change upon binding and the observed shift of the affinity curve upon Mn^{2+} activation strongly argue that ANG-2 activation of integrins occurs at sites of active integrin expression as in angiogenic tip cells (39).

Integrins $\alpha_v\beta_3$, $\alpha_v\beta_5$, and $\alpha_5\beta_1$ are arginine–glycine–aspartic acid (RGD) integrins interacting with the RGD binding motif in extracellular matrix molecules such as fibronectin and vitronectin.

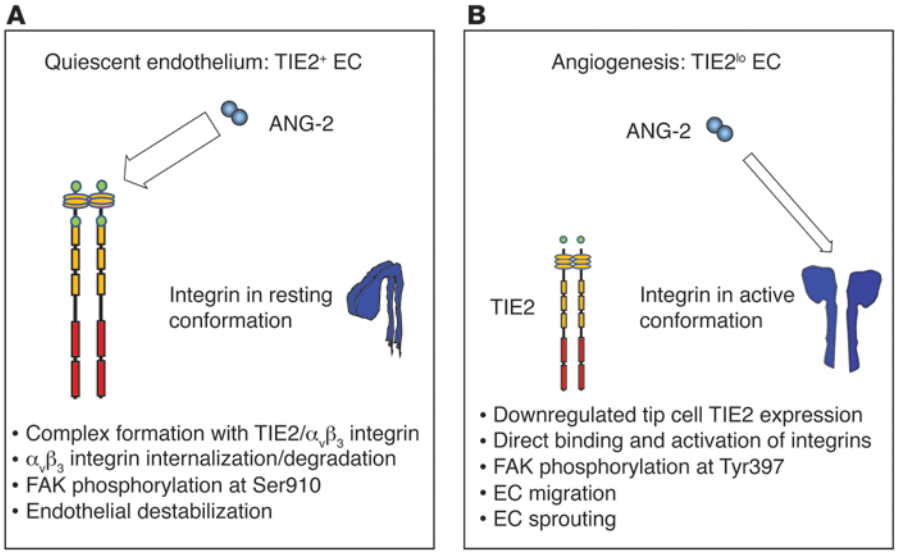

Figure 9
Model of the contextual bifunctional effects of ANG-2 during angiogenesis. (**A**) Quiescent resting ECs express TIE2. EC activation leads to secretion of Weibel-Palade body–stored ANG-2 and strong transcriptional ANG-2 upregulation. ANG-2 interferes with ANG-1–induced TIE2 activation to destabilize the resting EC monolayer and primes it to respond to exogenous cytokines. Endothelial destabilization is at least in part mediated by ANG-2/TIE2/integrin complex formation, which subsequently leads to FAK phosphorylation at Ser910, as well as integrin internalization and degradation (14). Thus, among the effects of ANG-2, the antagonistic mode of action predominates in resting ECs. (**B**) Angiogenic activation has a negative effect on EC TIE2 expression. As a result, angiogenic tip cells are TIE2 low or negative, whereas remodeling stalk and phalanx cells express TIE2. Conversely, expression of the integrins $\alpha_v\beta_3$, $\alpha_v\beta_5$, and $\alpha_5\beta_1$ is upregulated on angiogenic ECs. In the absence of TIE2, ANG-2 directly binds and activates integrins, which are in their conformationally active state in angiogenically activated ECs. Integrin activation induces FAK phosphorylation at Tyr397, Rac1 activation, and EC migration. As a result, the combination of differential receptor expression and affinity controls the net outcome of ANG-2 signaling. This allows ANG-2 to control different steps of the angiogenic cascade in a bifunctional manner.

Yet RGD-independent binding sites have been described (44). We therefore examined the ability of ANG-2 to interfere with fibronectin or vitronectin binding (Figure 7F). ANG-2 stimulation of ECs inhibited binding neither to fibronectin nor to vitronectin, implying that the ANG-2 integrin binding site is an RGD-independent domain. Interestingly, ANG-2 stimulation significantly promoted EC binding to fibronectin but not to vitronectin.

In order to investigate the binding of ANG-2 to $\alpha_v\beta_3$, $\alpha_v\beta_5$, and $\alpha_5\beta_1$ integrins in the absence of its cognate endothelial receptor TIE2, we next studied the adhesion of lentivirally silenced TIE2^{lo} ECs to immobilized ANG-2. These experiments revealed a more pronounced adhesion-blocking effect of the $\alpha_v\beta_3$ and $\alpha_5\beta_1$ antibodies in the absence of TIE2 (Figure 7G). The combination of $\alpha_v\beta_3$, $\alpha_v\beta_5$, and $\alpha_5\beta_1$ integrin antibodies reduced adhesion of TIE2^{lo} ECs to background levels (Figure 7G), implying that TIE2 and the integrins $\alpha_v\beta_3$, $\alpha_v\beta_5$, and $\alpha_5\beta_1$ act as the 4 main receptors for ANG-2 in ECs.

TIE2^{lo} ECs express $\alpha_v\beta_3$, $\alpha_v\beta_5$, and $\alpha_5\beta_1$ integrins during angiogenesis. The integrins $\alpha_v\beta_3$, $\alpha_v\beta_5$, and $\alpha_5\beta_1$ have previously been associated with the angiogenic EC phenotype (39). We consequently probed the expression of these integrins in the different models of TIE2^{hi} and TIE2^{lo} ECs employed in this study. All three integrins were detected in subconfluent and confluent ECs on the mRNA as well as on the protein level (Supplemental Figure 9). Likewise, mRNA content for the α_v, α_5, β_1, and β_3 subunits as well as the $\alpha_v\beta_3$, $\alpha_v\beta_5$, and $\alpha_5\beta_1$ protein heterodimers was detected on ECs in the spheroid sprouting angiogenesis assay (Supplemental Figure 10, A–C). Expression levels of these integrins did not change significantly during angiogenic activation. Furthermore, the expression was not altered in lentivirally silenced TIE2^{lo} ECs (Supplemental Figure 10D). Importantly, while the integrins were weakly expressed to barely detectable in microvessels of the adult skin (Supplemental Figure 11, A–C), all three integrins were prominently expressed in TIE2^{lo} ECs in human melanoma specimens (Supplemental Figure 11, D–F). β_1 Integrin expression has recently been reported in tip cells of the developing retina (16) and a recent publication indicates that $\alpha_5\beta_1$ is strongly expressed by angiogenic tip cells (45). Consistent with these findings, we detected $\alpha_v\beta_3$ integrin expression by all ECs in the vascular plexus of the developing retina (Supplemental Figure 11, G–I). These findings confirm previous reports of an association of $\alpha_v\beta_3$, $\alpha_v\beta_5$, and $\alpha_5\beta_1$ expression with the angiogenic EC phenotype (39) and establish the counterregulatory expression of TIE2 and the integrins $\alpha_v\beta_3$, $\alpha_v\beta_5$, and $\alpha_5\beta_1$ on quiescent and angiogenically activated ECs (as recently shown for $\alpha_v\beta_3$ integrin; ref. 22).

ANG-2–induced enhancement of VEGF sprouting and FAK (Tyr397) phosphorylation requires $\alpha_v\beta_3$, $\alpha_v\beta_5$, and $\alpha_5\beta_1$ integrins. ANG-2 stimulation of TIE2^{lo} ECs resulted in an angiogenic EC phenotype characterized by vascular sprouting, EC migration, and FAK (Tyr397) phosphorylation (Figures 3–5). At the same time, ANG-2 directly associated with the three angiogenic integrins, $\alpha_v\beta_3$, $\alpha_v\beta_5$, and $\alpha_5\beta_1$, with weaker affinity compared with TIE2 (Figures 6 and 7). Therefore, we next studied ANG-2–induced angiogenic effects for the requirement of $\alpha_v\beta_3$, $\alpha_v\beta_5$, and $\alpha_5\beta_1$ integrins in the spheroid sprouting angiogenesis assay. Corresponding to the results of the combined VEGF/ANG-2 stimulation experiments in the cornea pocket assay (Supplemental Figure 8A), ANG-2 enhanced sprouting angiogenesis of low VEGF–induced spheroid sprouting (Figure 8A, bar 4 vs. 2). This enhancing effect could be completely blocked with the ANG-2 neutralizing antibody (Supplemental Figure 12). The enhancing effect of ANG-2 on VEGF-induced sprouting angiogenesis was independent of TIE2, as it was also observed in TIE2-silenced ECs (Figure 8A, bar 10 vs. 8). Importantly, the ANG-2 effect could be blocked with the antibody cocktail against the integrins $\alpha_v\beta_3$, $\alpha_v\beta_5$, and $\alpha_5\beta_1$ (Figure 8A, bar 6 vs. 4 and bar 12 vs. 10).

Next, we examined whether the observed effect of p-FAK (Tyr397) is integrin dependent. Toward this end, we performed comparative integrin signaling experiments in TIE2^{hi} and TIE2^{lo} ECs. Adhesion of TIE2^{lo} ECs to an immobilized ANG-2 matrix led

to Mn^{2+}-dependent phosphorylation of FAK (Tyr397) (Figure 8B, lane 10 vs. 13 [ANG-2 effect], lane 10 vs. 8 [Mn^{2+} effect]). The integrin dependence of ANG-2–induced FAK phosphorylation was confirmed by a marked inhibitory effect of preincubating the cells with the $\alpha_v\beta_3$, $\alpha_v\beta_5$, and $\alpha_5\beta_1$ integrin antibody cocktail prior to ANG-2 stimulation (Figure 8B, lane 10 vs. 11). The integrin dependence of ANG-2–induced FAK phosphorylation was further corroborated by the demonstration that $TIE2^{hi}$ ECs did not respond to ANG-2 stimulation with increased FAK phosphorylation (Figure 8B, lane 3 vs. 6). Likewise, the integrin antibody cocktail did not affect FAK phosphorylation in the presence of ANG-2 (Figure 8B, lane 3 vs. 4). Based on these findings, we studied whether FAK (Tyr397) phosphorylation was also detectable during sprouting angiogenesis and could be inhibited by the integrin cocktail (Figure 8C). ANG-2 in combination with subcritical VEGF-induced sprouting was accompanied by strong FAK (Tyr397) phosphorylation at the edge of TIE2-silenced sprouting ECs (Figure 8C). Thus, EC sprouting and FAK (Tyr397) phosphorylation were inhibited by the integrin cocktail (Figure 8C). To translate the cellular experiments to an in vivo model of angiogenesis, we performed additional corneal pocket angiogenesis assays. These were done in the presence or absence of ANG-2, subcritical doses of VEGF, and the integrin cocktail (Figure 8D). FAK (Tyr397) phosphorylation upon ANG-2 and low-VEGF stimulation was blocked by treatment with the integrin antibody cocktail (Figure 8D).

Discussion

Genetic experiments have solidly established ANG-2 as an antagonistic TIE2 ligand negatively interfering with vessel stabilization and maturation by controlling the ANG-1/TIE2 axis (2, 9–12). However, recent studies have suggested that ANG-2 inhibition has more profound effects on angiogenesis than silencing of TIE2, indicating that ANG-2 may exert functions independent of its cognate receptor TIE2 (6). Correspondingly, a number of reports have shown that ANG-2 can under certain conditions activate ECs and exert proangiogenic effects, which is mechanistically and functionally difficult to relate to possible TIE2 activation (15, 46, 47). A mechanistic understanding of the contextual agonistic and antagonistic effects of ANG-2 on ECs has been enigmatic in the field of angiopoietin research, and its lack represents a major limitation for the rational exploitation of ANG-2 as a therapeutic target of antiangiogenic intervention. In this study, we show that (a) angiogenically activated endothelial tip cells are TIE2 negative (hereinafter referred to as $TIE2^{lo}$ ECs); (b) ANG-2 binds to $\alpha_v\beta_3$, $\alpha_v\beta_5$, and $\alpha_5\beta_1$ integrins with lower affinity than to TIE2; (c) ANG-2 induces FAK (Tyr397) phosphorylation and stimulates EC migration and sprouting in $TIE2^{lo}$ ECs in an integrin-dependent manner; and (d) ANG-2 inhibition interferes with angiogenesis, not only affecting remodeling of the TIE2-expressing stalk cell vasculature (21, 28), but also by impairing sprouting tip cell migration. Collectively, the data establish a contextual model whereby agonistic and antagonistic functions of ANG-2 are regulated by differential expression of and affinity for the cognate receptor TIE2 and the alternative integrin receptors, respectively (Figure 9).

ANG-2 has been identified as the second TIE2 ligand by homology screening. Genetic experiments have characterized ANG-2 as the functional antagonist of ANG-1/TIE2 signaling. Yet solid biochemical data indicating that ANG-2 interferes negatively with ANG-1–induced TIE2 phosphorylation in cellular models are scant (48). Still, several studies have reported that ANG-2 can induce TIE2 phosphorylation in cultured ECs (47, 48).

An important aspect in understanding the complexity of angiopoietin biology is a critical appreciation of the distinct differences in ligand production and presentation. While ANG-1 is produced by numerous cell types including mural cells (pericytes, smooth muscle cells), fibroblasts, and monocytes, thereby acting in a paracrine manner, ANG-2 is almost exclusively produced by ECs. Correspondingly, the genetic overexpression of ANG-2 in ECs in vivo provided the hitherto most unambiguous evidence for a receptor activation–inhibiting function of ANG-2 (12). In line with an antagonistic mode of action of ANG-2 on TIE2-expressing ECs, experiments in ANG-2–deficient mice have established a role of ANG-2 in facilitating cytokine-controlling EC responsiveness to angiogenic and inflammatory stimuli (3, 28). Taken together, overwhelming evidence supports the concept that autocrine-acting ANG-2 serves as antagonistic ligand in TIE2-expressing cells. In contrast, there is presently no definite data supporting a TIE2 receptor–activating role of EC-derived ANG-2 in vivo.

ANG-2 is expressed at low levels in resting ECs. It is stored in Weibel-Palade bodies, from which it can be secreted in seconds to minutes to control ultra-rapid EC responses. Angiogenic EC activation leads to dramatic transcriptional upregulation of ANG-2 expression, with most pronounced upregulation in migrating and invading EC tip cells (16, 17). The discovery of the strong downregulation of TIE2 below the detection level in tip cells (Figure 2) consequently provoked the hypothesis that ANG-2 is regulating autocrine functions in angiogenic ECs in a TIE2-independent manner. This study was therefore aimed at delineating in detail the role of ANG-2 in $TIE2^{lo}$ ECs. It deliberately did not focus on ANG-1, since (a) ANG-1 is weakly expressed by ECs, if at all; and (b) the ANG-2/ANG-1 ratio is shifted toward ANG-2 during angiogenesis. For these reasons ANG-2, but not ANG-1, is a primary autocrine candidate regulator of the angiogenic tip cell phenotype.

Confirming and extending previous studies in non-ECs (23, 34–37), we could show that ANG-2 directly binds the integrins $\alpha_v\beta_3$, $\alpha_v\beta_5$, and $\alpha_5\beta_1$. Most notably, though, systematic comparative binding experiments revealed a lower binding affinity of these integrins to ANG-2 compared with TIE2. This differential receptor affinity validated TIE2 as the primary high-affinity receptor of ANG-2. Yet it also suggested that ANG-2 may be able to bind and activate integrins in TIE2-negative ECs. Based on these concepts, we performed systematic comparative expression profiling experiments involving TIE2 and the ANG-2–binding integrins in different cellular models and in physiological and pathological angiogenesis settings. These experiments established a differential expression pattern of TIE2 and the ANG-2–binding integrins: TIE2 was prominently expressed in resting ECs and downregulated in angiogenic ECs, while $\alpha_v\beta_3$, $\alpha_v\beta_5$, and $\alpha_5\beta_1$ integrins had a counterregulatory expression pattern, with most the pronounced expression in angiogenic ECs (see also ref. 39 for review on angiogenic integrins).

The integrins $\alpha_v\beta_3$, $\alpha_v\beta_5$, and $\alpha_5\beta_1$ are primarily RGD integrins interacting with the RGD binding motif but may also show RGD-independent binding (4). ANG-2 contains no RGD binding motif, and competition experiments did not reveal decreased binding to RGD proteins (fibronectin or vitronectin) in the presence of ANG-2. Instead, ANG-2/integrin binding was enhanced by cations, implying that the MIDAS of the I-like domain is involved in ANG-2 integrin adhesion. The integrins $\alpha_v\beta_3$, $\alpha_v\beta_5$, and $\alpha_5\beta_1$ do not contain an α I-like domain. Therefore, it appears most likely that the β I-like domain is involved in ANG-2/integrin binding (43).

The β I-like domain is only accessible when the integrin is expressed in its high-affinity conformation (49), suggesting that the ANG-2/integrin link requires the active conformation of the integrins. This is also supported by the recent report demonstrating ANG-2 binding to $\alpha_5\beta_1$ integrin only when the β_1 subunit is expressed in its high-affinity conformation (38).

ANG-2 induces FAK (Tyr397) phosphorylation and sprouting and migration of $TIE2^{lo}$ ECs. This activating phenotype is in sharp contrast to the effect of ANG-2 in TIE2-expressing ECs. ANG-2 binding of TIE2 in resting ECs leads to the formation of an ANG-2/TIE2/integrin complex with FAK (Ser910) phosphorylation and subsequent focal adhesion disassembly as well as integrin endocytosis and degradation (14). Moreover, integrin function during angiogenesis itself is also highly complex and contextual. It is critically regulated by dosage effects (e.g., as shown for $\alpha_v\beta_3$ and $\alpha_v\beta_5$; ref. 50), and compensatory mechanisms also play a role (40). Yet a proangiogenic function of the ANG-2/integrin interaction is supported not only by the preferential tip cell expression of ANG-2 binding integrins and the pro-migratory effects in cellular models, but most importantly by the tip cell phenotype–inhibiting effects of ANG-2 blockade during angiogenesis in vivo.

In summary, the present study provides a model that accounts for the complexity of ANG-2 functions during angiogenesis (Figure 9). It explains direct proangiogenic effects of ANG-2 by binding of integrins. These are expressed by invading and migrating tip cell ECs, which themselves downregulate TIE2 expression. In turn, stalk and phalanx cells during vascular remodeling and differentiation engage in ANG-1/TIE2 signaling, which ANG-2 impacts in an antagonistic, destabilizing manner. As such, ANG-2 can be considered as a double-edged sword, controlling angiogenesis in a bivalent manner depending on the absence or presence of TIE2.

Methods

Materials. See Supplemental Experimental Procedures for details and sources of recombinant proteins, antibodies, and cells employed in this study.

Studies with clinical specimens. Clinical specimens of malignant melanoma were obtained from Jochen Utikal from the Department of Dermatology, Venerology and Allergology, Medical Faculty Mannheim, Heidelberg University.

Animal experiments. The genetic background of all mice used was C57BL/6. The human xenograft endothelial assay was performed as described previously (30, 31).

Lentiviral and/or adenoviral transduction. See Supplemental Experimental Procedures for details or lentiviral and adenoviral transduction protocols.

Pull-down analysis. Double-transduced HUVECs were grown subconfluent to 70%–80% on fibronectin-coated wells. Cells were lysed with GST-FISH buffer (50 mM Tris-HCl, 150 mM NaCl, 4 mM $MgCl_2$, 10% glycerine, 1% Igepal CA 630) and precleared by centrifugation. Thereafter, activated Rac1-GTP was precipitated with sepharose-bound purified GST fusion proteins containing the Rac-binding domain of PAK1. After separation by 15% SDS-PAGE, the amount of activated and total Rac1 was analyzed by immunoblotting.

Adhesion assay. Adhesion assays were performed in a flat-bottom 96-well plate format (Costar, no. 3595). ANG-2, which had been reconstituted according to the manufacturer's instructions, was used for coating of the wells. The wells were either coated with ANG-2 diluted in PBS overnight at 4°C or with fibronectin for 1 hour at 37°C. After coating, the wells were blocked in PBS plus 3% BSA (heat-inactivated; 37°C; 30 minutes) and finally washed 3 times with PBS and kept in PBS until cells were prepared for the assay. Cells were suspended in EBM plus 0.1% BSA at a concentration of 10^6 cells. If cells were preincubated with, e.g., antibodies, they were suspended in EBM plus 0.2% BSA with or without 2 mM $MnCl_2$. The antibodies were diluted in EBM, and equal volumes of cells and antibody solution were mixed. Cells were plated at 50,000 cells or 50 μl per well and allowed to adhere (37°C; 5% CO_2; 40 minutes). Wells were washed with PBS once to remove non-adherent cells. Adherent cells were stained with 50 μl crystal violet (0.1% in H_2O; 5 minutes; room temperature). Crystal violet was removed, and wells were allowed to dry following 3 washes before 100 μl methanol was added per well. Color intensity was measured at 550 nm. Fibronectin-coated (100 μg/ml) and uncoated wells (blocking only: BSA controls) were used as positive and negative adhesion controls, respectively.

Adhesion assay and Western blot analysis. Adhesion assays were performed as described above. PBS (100 μl) containing 500 μM orthovanadate was added to the wells, and unattached cells were removed and collected by centrifugation (5 minutes; 400 *g*; 4°C) and lysed in lysis buffer. Adherent cells were incubated with 60 μl SDS sample buffer containing 500 μM orthovanadate and 1% (v/v) protease inhibitor mix (SERVA; 5 minutes; room temperature). Finally, the pellets from unattached cells and the lysis solution from attached cells were pooled. Discontinuous 10% SDS-PAGE was performed, followed by Western blotting.

ANG-2 integrin binding in ECs. ECs with lentivirus-mediated overexpression of ANG-2 and silenced for TIE2 receptor were allowed to grow to confluence in 10-cm dishes. Medium was not changed at least 3 days prior to cell lysis. Cells were lysed with 1.0 ml NP40 buffer (1 M Tris-HCl, 5 M NaCl, 2 ml NP40 dilution, 250 mM EDTA, 20 ml glycerine, protease inhibitor cocktail [SERVA] in H_2O), and immunoprecipitation was performed with the indicated antibody (2 μg/) with G-sepharose overnight at 4°C. The immunoprecipitate was centrifuged for 2 minutes at 1,000 *g*, washed 3 times with PBS, boiled with 5× sample buffer, and analyzed by SDS-PAGE and Western blotting.

ANG-2 integrin binding Western blot analysis in a cell-free system. Purified undiluted integrin protein (5 μl), 30 μl ANG-2 (10 μg/ml), and 2 μg of the corresponding integrin antibody were incubated with G-sepharose in 1.0 ml NP40 buffer (1 M Tris-HCl, 5 M NaCl, 2 ml NP40 dilution, 250 mM EDTA, 20 ml glycerine, protease inhibitor cocktail [SERVA] in H_2O) overnight at 4°C. ANG-2 incubated with IgG antibody or ANG-2, integrin, and IgG antibody were used as controls. The immunoprecipitate was centrifuged for 2 minutes at 1,000 *g*, washed 3 times with PBS, boiled with 5× sample buffer, and analyzed by SDS-PAGE and Western blotting.

ANG-2 integrin binding ELISA. Equal amounts of TIE2 and integrin per well were used for the coating of F-bottom, medium binding ELISA plates (Greiner; overnight at 4°C). Heat-inactivated BSA (3% in 50 μl bicarbonate buffer [0.08 g Na_2CO_3, 0.14 g $NaHCO_3$ in 50 ml distilled H_2O]) was used as control. Wells were washed intensely with PBS (containing 1 mM Mn^{2+}) and blocked with freshly dissolved heat-inactivated 1% casein with 1 mM Mn^{2+} for 120 minutes at room temperature. After intense washing with TBS at the indicated pH, biotinylated ANG-2 (400 ng/ml) was applied for 2 hours in TBS at the indicated pH, 1 mM Mn^{2+}, 1 mM Ca^{2+}, and proteinase inhibitor and incubated overnight. Wells were washed 3 times with TBS (with 1 mM Mn^{2+}, 1 mM Ca^{2+}). Samples were subjected to 2.5% glutaraldehyde fixation for 10 minutes, followed by intense washing with TBS (Mn^{2+}, Ca^{2+}). Streptavidin-HRP (Zymed, Invitrogen) was added for 45 minutes at room temperature. After 3 washes with NP40 buffer, an ELISA kit (BD OptEIA) was applied, and chemiluminescence was measured at 405 nm.

Spheroid-based sprouting assay. HUVECs were suspended in 80% ECGM/20% Methocel medium and plated in droplets of 25 μl and 400 cells. After the spheroids were harvested with 10% FCS in PBS, they were centrifuged (300 *g*; 5 minutes), the supernatant was removed, and the spheroids were resuspended in 80% Methocel and 20% FCS. An equal volume of collagen mixture (1:2 in 0.1% acetic acid; 1× Medium 199; 50 mM HEPES;

neutralized with 0.2 M NaOH) was added prior to pouring the spheroid suspension into 24-well plates. The gels were allowed to solidify (37°C; 30 minutes). If required, VEGF was added at a concentration of 50 ng/ml. Next, spheroids were incubated to allow sprouting angiogenesis (37°C; 5% CO_2; 24 hours).

Digestion of spheroids for flow cytometric analysis. All experimental steps were performed on ice. Spheroid-containing gels were diluted and solubilized with an equal volume of PBS and pooled into 15-ml Falcon tubes. For washings, the Falcon tubes were filled completely with PBS and centrifuged (300 *g*; 5 minutes; 4°C). Supernatants were removed without disruption of the soft layer of the gel. Washings were repeated 3 times in order to remove FCS components in the gel. A collagenase digestion mixture (125 U/ml collagenase I [Sigma-Aldrich], 125 U/ml collagenase II [Biochrom], 50 μg/ml Liberase TM [Roche], 1 U/ml dispase [Roche]) was added to the gel and incubated (300 *g*; 5 minutes; 4°C). After centrifugation (300 *g*; 5 minutes; 4°C) and removal of the supernatants, trypsin was added to the spheroids and incubated (37°C; 200 *g*; 3 minutes). The reaction was stopped by addition of cold FACS buffer (10% FCS, 1% NaN_3 in PBS). The single-cell suspension was incubated in FACS buffer (4°C; 10 minutes).

Flow cytometric analysis. Cells were transferred into U-shaped-bottom 96-well plates at a density of 100,000 cells per well. Cells were incubated with primary antibodies against TIE2, integrins, mouse IgG, or goat IgG diluted in FACS buffer (10% FCS, 1% NaN_3 in PBS; 30 minutes; 4°C; 50 μl per well). After washing with FACS buffer, secondary and isotype control antibodies in FACS buffer were incubated for 15 minutes at 4°C and in the dark. Cells were washed twice with FACS buffer prior to measurement. Cells were gated to exclude dead cells, debris, and cell aggregates. Median fluorescence intensity values were used for data analysis.

Scratch wound assay. Virally transduced HUVECs were grown to confluence on fibronectin-coated (5 μg/ml in PBS; 1 hour; 37°C) glass slides (Labtek). The scratch was manually set with the tip of a pipette. For time-lapse video microscopy with periods of observation for 18 hours, a Cell Observer microscope (Zeiss) was used. Pictures were taken every 15 minutes.

Single-cell migration assay. Glass slides (16-well; Labtek) were coated with fibronectin (5 μg/ml in PBS; 1 hour; 37°C). To achieve sufficient ANG-2 concentrations, the supernatant from a confluent monolayer of double-transduced HUVECs was taken prior to the migration experiment and stored on ice. The double-transduced cells were suspended in ECGM complete medium (5,000 cells/ml), and 150 μl was added per well. Cells were allowed to adhere for 2 hours. The cell density after adhesion was about 5%–10% confluence. In order to guarantee sufficient ANG-2 in the medium to elicit a migratory response, ECGM complete was exchanged with the cells' supernatants (see above). The supernatants themselves were tested for ANG-2 expression by ELISA. Cells were observed for 20–24 hours with intervals between frames of 8–10 minutes by time-lapse video microscopy.

Automated cell tracking and data refinement. See Supporting Experimental Procedures for details on the automated cell tracking protocols (Supplemental Table 1).

TIE2 ± CD34/CD31 ± integrin ± FAK (Tyr397) staining protocol and retinal immunohistochemical studies. See Supplemental Experimental Procedures for details on retina sample processing and details of TIE2, CD34, and integrin single, double, and triple stainings.

ANG-2 in situ hybridization and collagen immunohistochemistry studies. See Supplemental Experimental Procedures for details on retina sample processing and details.

Statistics. Data are presented as mean ± SD unless otherwise indicated. Differences between experimental groups were analyzed by 2-tailed Student's *t* test if not otherwise specified. A *P* value less than 0.05 was considered statistically significant.

Study approval. Studies with melanoma specimens were approved by the local ethic committee (Medizinischen Ethik-Kommission II, UMM; 2009-350N-MA), with written informed consent received from donors. All animal procedures were approved by the local government authorities (Regierungspräsidium Karlsruhe, AZ 35-9185-81/G-15-07 and /G-77-06).

Acknowledgments

This work was supported by grants from the German Research Council (DFG SFB-TR23 [Vascular Differentiation and Remodeling], project A2 [to E. Chavakis], A3 [to H.G. Augustin], B1 [to S. Goerdt], and B6 [to T. Wieland]; DFG SFB-873 [Maintenance and Differentiation of Stem Cells], project B6 [to H.G. Augustin]; DFG SFB-TR77 [Liver Cancer], project C3 [to H.G. Augustin and S. Goerdt]). H.G. Augustin is supported by an endowed chair from the Aventis Foundation. We thank Stella Hertel and Doris Baltus for excellent technical assistance. We thank Felix Bestvater and Manuela Brom (Light Microscopy Core Facility, German Cancer Research Center Heidelberg) for help with confocal microscopy.

Received for publication January 31, 2012, and accepted in revised form April 4, 2012.

Address correspondence to: Hellmut G. Augustin, Joint Research Division of Vascular Biology, Medical Faculty Mannheim (CBTM), Heidelberg University, and German Cancer Research Center Heidelberg (DKFZ-ZMBH Alliance), Im Neuenheimer Feld 280, D-69221 Heidelberg, Germany. Phone: 49.6221.421500; Fax: 49.6221.421515; E-mail: augustin@angiogenese.de.

1. Augustin HG, Koh GY, Thurston G, Alitalo K. Control of vascular morphogenesis and homeostasis through the angiopoietin-Tie system. *Nat Rev Mol Cell Biol*. 2009;10(3):165–177.
2. Gale NW, et al. Angiopoietin-2 is required for postnatal angiogenesis and lymphatic patterning, and only the latter role is rescued by Angiopoietin-1. *Dev Cell*. 2002;3(3):411–423.
3. Fiedler U, et al. Angiopoietin-2 sensitizes endothelial cells to TNF-alpha and has a crucial role in the induction of inflammation. *Nat Med*. 2006; 12(2):235–239.
4. Koh YJ, et al. Double antiangiogenic protein, DAAP, targeting VEGF-A and angiopoietins in tumor angiogenesis, metastasis, and vascular leakage. *Cancer Cell*. 2010;18(2):171–184.
5. Huang H, Bhat A, Woodnutt G, Lappe R. Targeting the ANGPT-TIE2 pathway in malignancy. *Nat Rev Cancer*. 2010;10(8):575–585.
6. Mazzieri R, et al. Targeting the ANG2/TIE2 axis inhibits tumor growth and metastasis by impairing angiogenesis and disabling rebounds of proangiogenic myeloid cells. *Cancer Cell*. 2011; 19(4):512–526.
7. Dumont DJ, et al. Dominant-negative and targeted null mutations in the endothelial receptor tyrosine kinase, tek, reveal a critical role in vasculogenesis of the embryo. *Genes Dev*. 1994;8(16):1897–1909.
8. Sato TN, et al. Distinct roles of the receptor tyrosine kinases Tie-1 and Tie-2 in blood vessel formation. *Nature*. 1995;376(6535):70–74.
9. Suri C, et al. Requisite role of angiopoietin-1, a ligand for the TIE2 receptor, during embryonic angiogenesis. *Cell*. 1996;87(7):1171–1180.
10. Hackett SF, Wiegand S, Yancopoulos G, Campochiaro PA. Angiopoietin-2 plays an important role in retinal angiogenesis. *J Cell Physiol*. 2002; 192(2):182–187.
11. Maisonpierre PC, et al. Angiopoetin-2, a natural antagonist for Tie2 that disrupt in vivo angiogenesis. *Science*. 1997;277(5322):55–60.
12. Reiss Y, et al. Angiopoietin-2 impairs revascularization after limb ischemia. *Circ Res*. 2007;101(1):88–96.
13. Scharpfenecker M, Fiedler U, Reiss Y, Augustin HG. The Tie-2 ligand angiopoietin-2 destabilizes quiescent endothelium through an internal autocrine loop mechanism. *J Cell Sci*. 2005;118(pt 4):771–780.
14. Thomas M, et al. Angiopoietin-2 stimulation of endothelial cells induces alphavbeta3 integrin internalization and degradation. *J Biol Chem*. 2010; 285(31):23842–23849.
15. Daly C, et al. Angiopietin-2 functions as an autocrine protective factor in stressed endothelial cells. *Proc Natl Acad Sci U S A*. 2006;103(42):15491–15496.
16. Toro Rd, et al. Identification and functional analysis of endothelial tip cell-enriched genes. *Blood*. 2010; 116(19):4025–4033.
17. Strasser GA, Kaminker JS, Tessier-Lavigne M. Microarray analysis of retinal endothelial tip cells identifies CXCR4 as a mediator of tip

cell morphology and branching. *Blood*. 2010; 115(24):5102–5110.
18. Tanaka S, et al. Tie2 vascular endothelial receptor expression and function in hepatocellular carcinoma. *Hepatology*. 2002;35(4):861–867.
19. Hida K, et al. Tumor-associated endothelial cells with cytogenetic abnormalities. *Cancer Res*. 2004; 64(22):8249–8255.
20. Fathers KE, et al. Heterogeneity of Tie2 expression in tumor microcirculation: influence of cancer type, implantation site, and response to therapy. *Am J Pathol*. 2005;167(6):1753–1762.
21. Hashizume H, et al. Complementary actions of inhibitors of angiopoietin-2 and VEGF on tumor angiogenesis and growth. *Cancer Res*. 2010; 70(6):2213–2223.
22. Pan D, et al. Molecular photoacoustic imaging of angiogenesis with integrin-targeted gold nanobeacons. *FASEB J*. 2011;25(3):875–882.
23. Carlson TR, Feng Y, Maisonpierre PC, Mrksich M, Morla AO. Direct cell adhesion to the angiopoietins mediated by integrins. *J Biol Chem*. 2001; 276(28):26516–26525.
24. Serini G, Napione L, Arese M, Bussolino F. Besides adhesion: new perspectives of integrin functions in angiogenesis. *Cardiovasc Res*. 2008;78(2):213–222.
25. Schaefer W, et al. Immunglobulin domain crossover as a generic approach for the production of bispecific IgG antibodies. *Proc Natl Acad Sci U S A*. 2011;108(27):11187–11192.
26. Rennel ES, Regula JT, Harper SJ, Thomas M, Klein C, Bates DO. A human neutralizing antibody specific to Ang-2 inhibits ocular angiogenesis. *Microcirculation*. 2011;18(7):598–607.
27. Abai B, Thayer D, Glat PM. The use of a dermal regeneration template (Integra) for acute resurfacing and reconstruction of defects created by excision of giant hairy nevi. *Plast Reconstr Surg*. 2004;114(1):162–168.
28. Nasarre P, et al. Host-derived angiopoietin-2 affects early stages of tumor development and vessel maturation but is dispensable for later stages of tumor growth. *Cancer Res*. 2009;69(4):1324–1333.
29. Wong AL, Haroon ZA, Werner S, Dewhirst MW, Greenberg CS, Peters KG. Tie2 expression and phosphorylation in angiogenic and quiescent adult tissues. *Circ Res*. 1997;81(4):567–574.
30. Alajati A, et al. Spheroid-based engineering of a human vasculature in mice. *Nat Methods*. 2008; 5(5):439–445.
31. Laib AM, Bartol A, Alajati A, Korff T, Weber H, Augustin HG. Spheroid-based human endothelial cell microvessel formation in vivo. *Nat Protoc*. 2009; 4(8):1202–1215.
32. Korff T, Kimmina S, Martiny-Baron G, Augustin HG. Blood vessel maturation in a 3-dimensional spheroidal coculture model: direct contact with smooth muscle cells regulates endothelial cell quiescence and abrogates VEGF responsiveness. *FASEB J*. 2001;15(2):447–457.
33. Petrie RJ, Doyle AD, Yamada KM. Random versus directionally persistent migration. *Nat Rev Mol Cell Biol*. 2009;10(8):538–549.
34. Bezuidenhout L, Zilla P, Davies N. Association of Ang-2 with integrin beta 2 controls Ang-2/PDGF-BB-dependent upregulation of human peripheral blood monocyte fibrinolysis. *Inflammation*. 2009;32(6):393–401.
35. Dallabrida SM, Ismail N, Oberle JR, Himes BE, Rupnick MA. Angiopoietin-1 promotes cardiac and skeletal myocyte survival through integrins. *Circ Res*. 2005;96(4):e8–24.
36. Hu B, Jarzynka MJ, Guo P, Imanishi Y, Schlaepfer DD, Cheng S-Y. Angiopoietin 2 induces glioma cell invasion by stimulating matrix metalloprotease 2 expression through the αvβ1 integrin and focal adhesion kinase signaling pathway. *Cancer Res*. 2006;66(2):775–783.
37. Imanishi Y, et al. Angiopoetin-2 stimulates breast cancer metastasis through the αvβ1 integrin-mediated pathway. *Cancer Res*. 2007;67(9):4254–4263.
38. Sun WY, Pitson SM, Bonder CS. Tumor necrosis factor-induced neutrophil adhesion occurs via sphingosine kinase-1-dependent activation of endothelial {alpha}5{beta}1 integrin. *Am J Pathol*. 2010; 177(1):436–446.
39. Desgrosellier JS, Cheresh DA. Integrins in cancer: biological implications and therapeutic opportunities. *Nat Rev Cancer*. 2010;10(1):9–22.
40. van der Flier A, et al. Endothelial alpha5 and alphav integrins cooperate in remodeling of the vasculature during development. *Development*. 2010;137(14):2439–2449.
41. Lenter M, Uhlig H, Hamann A, Jeno P, Imhof B, Vestweber D. A monoclonal antibody against an activation epitope on mouse integrin chain beta 1 blocks adhesion of lymphocytes to the endothelial integrin alpha 6 beta 1. *Proc Natl Acad Sci U S A*. 1993;90(19):9051–9055.
42. Luque A, Gomez M, Puzon W, Takada Y, Sanchez-Madrid F, Cabanas C. Activated conformations of very late activation integrins detected by a group of antibodies (HUTS) specific for a novel regulatory region (355-425) of the common beta 1 chain. *J Biol Chem*. 1996;271(19):11067–11075.
43. Takagi J. Structural basis for ligand recognition by integrins. *Curr Opin Cell Biol*. 2007;19(5):557–564.
44. Wang Z, et al. RGD-independent cell adhesion via a tissue transglutaminase-fibronectin matrix promotes fibronectin fibril deposition and requires syndecan-4/2 and {alpha}5{beta}1 integrin co-signaling. *J Biol Chem*. 2010;285(51):40212–40229.
45. Stenzel D, et al. Integrin-dependent and -independent functions of astrocytic fibronectin in retinal angiogenesis. *Development*. 2011;138(20):4451–4463.
46. Tressel SL, Huang RP, Tomsen N, Jo H. Laminar shear inhibits tubule formation and migration of endothelial cells by angiopoietin-2 dependent mechanisms. *Arterioscl Thromb Vasc Biol*. 2007; 27(10):2150–2156.
47. Yuan HT, Khankin EV, Karumanchi SA, Parikh SM. Angiopoietin 2 is a partial agonist/antagonist of Tie2 signaling in the endothelium. *Mol Cell Biol*. 2009; 29(8):2011–2022.
48. Saharinen P, et al. Angiopoietins assemble distinct Tie2 signalling complexes in endothelial cell-cell and cell-matrix contacts. *Nature Cell Biology*. 2008; 10(5):527–537.
49. Luo BH, Springer TA. Integrin structures and conformational signaling. *Curr Opin Cell Biol*. 2006; 18(5):579–586.
50. Reynolds AR, et al. Stimulation of tumor growth and angiogenesis by low concentrations of RGD-mimetic integrin inhibitors. *Nat Med*. 2009; 15(4):392–400.